Exploration and Mining Geology, Vol. 16, Nos. 3–4, p. 209–232, 2007

0964-1823/00 $17.00 + .00

A Review of Iron Oxide Copper-Gold Deposits, with Focus on the Wernecke Breccias, Yukon, Canada, as an Example of a Non-Magmatic End Member and Implications for IOCG Genesis and Classification

J.A. HUNT[1,2,3,†] , T. BAKER[2], AND D.J. THORKELSON[4]

(Received February 16, 2006; accepted August 25, 2007)

Abstract — New data indicate Wernecke Breccia-associated iron oxide copper-gold (IOCG) deposits likely formed from moderate-temperature, high-salinity, non-magmatic brines. The breccias formed in an area underlain by a sedimentary sequence that locally contained evaporites (potential source of chloride and possibly sulfur) and was thick enough to produce elevated fluid temperatures. Metals (Fe, Cu, Co, U) were probably derived from host strata, transported as chloride complexes, and precipitated due to changes in fluid temperature and pressure during brecciation. These new data suggest that the spectrum of genetic models for IOCG deposits that typically invoke formation from magmatic or hybrid magmatic–non-magmatic fluids should be expanded to include those systems that formed in a non-magmatic environment. Modifications to the definition of IOCG systems are proposed that reflect the degree of involvement of magmatic and/or non-magmatic fluids and the nature of the mineralizing environment. A division into magmatic, non-magmatic, and hybrid magmatic–non-magmatic IOCG types is suggested. Typical magmatic end-member IOCG deposits include Lightning Creek and Eloise, Australia. Hybrid magmatic–non-magmatic IOCG examples include Ernest Henry and Olympic Dam, Australia. The Wernecke Breccia and Redbank deposits are suggested as possible representatives of non-magmatic IOCG end members. End-member magmatic IOCG deposits have similarities to some porphyry deposits, whereas non-magmatic IOCG end members share characteristic with some sediment-hosted Cu deposits, suggesting that the range of IOCG deposits may form a link between intrusive- and sediment-related deposits.

Key Words: IOCG, Wernecke Breccias, iron oxide copper-gold deposits, Yukon, Proterozoic.

Sommaire — De nouvelles données indiquent que les gîtes d'oxyde de fer-cuivre-or de type IOCG associés à la brèche de Wernicke se sont vraisemblablement formés à partir de saumures non-magmatiques de température modérée et de grande salinité. Les brèches se sont formées dans une région sous-tendue par une séquence sédimentaire contenant localement des évaporites (source potentielle de chlore et possiblement de souffre) dont l'épaisseur était suffisamment importante pour produire un fluide à température élevée. Les métaux (Fe, Cu, Co, U) ont probablement été dérivés des strates encaissantes, transportés sous formes de complexes de chlorures et précipités conséquemment à des changements dans la température et la pression du fluide durant la bréchification. Ces nouvelles données suggèrent que le spectre de modèles génétiques pour les gîtes de type IOCG qui font typiquement appel à des fluides magmatiques ou à des fluides hybrides magmatiques-non-magmatiques devrait être élargi pour inclure les systèmes formés dans un environnement non-magmatique. Des modifications sont proposées à la définition des systèmes IOCG afin de refléter le degré d'implication des fluides magmatiques et/ou non-magmatiques et la nature de l'environnement minéralisant. Une division des gîtes IOCG en types magmatiques, non-magmatiques et hybrides magmatiques-non-magmatiques est suggérée. Des gîtes IOCG typiques du pôle magmatique comprennent Lightning Creek et Eloise, en Australie. Des exemples de gîtes hybrides magmatiques-non-magmatiques incluent Ernest Henry et Olympic Dam, en Australie. Les gîtes de la brèche de Wernecke et Redbank sont proposés comme représentant possibles pour le pôle non-magmatique du spectre des gîtes IOCG. Les gîtes de type IOCG au pôle magmatique du spectre présentent des similarités avec certains gîtes de type porphyrique, alors que les gîtes de types IOCG situés au pôle non-magmatique du spectre partagent des caractéristiques avec certains gîtes de cuivre à encaissant sédimentaire, ce qui suggère que l'éventail des types de gîte IOCG relie les gîtes d'affinités magmatique et sédimentaire..

---

[1] Yukon Geological Survey, Whitehorse, Yukon, Y1A 2C6.
[2] Economic Geology Research Unit, James Cook University, Queensland, Australia, 4811.
[3] *Currently at* CODES, University of Tasmania, Private Bag 79, Hobart, Tasmania, Australia, 7001.
[4] Department of Earth Sciences, Simon Fraser University, Burnaby, British Columbia, V5A 1S6.

[†] *Corresponding Author:* E-mail: julie.hunt@utas.edu.au

Introduction

The discovery of the giant Olympic Dam deposit (Fig. 1, Table 1) in the 1970s and the ensuing increase in exploration and research aimed at the discovery of similar deposits, led to proposals for a new deposit class: iron oxide (Cu-U-Au-rare earth elements (REE)) deposits (e.g., Meyer, 1988; Einaudi and Oreskes, 1990; Gandhi and Bell, 1990). A description of general characteristics was first published in Hitzman et al. (1992), based largely on studies of Olympic Dam and prospects in the Stuart Shelf (Australia), the Kiruna district (Sweden), the southeast Missouri iron district (USA), and the Wernecke Breccias (Canada). The definition was refined in Hitzman (2000) and Kiruna-type magnetite-apatite deposits were no longer included; instead magnetite-apatite and iron oxide Cu-Au (IOCG) deposits were considered to form end members of a continuum.

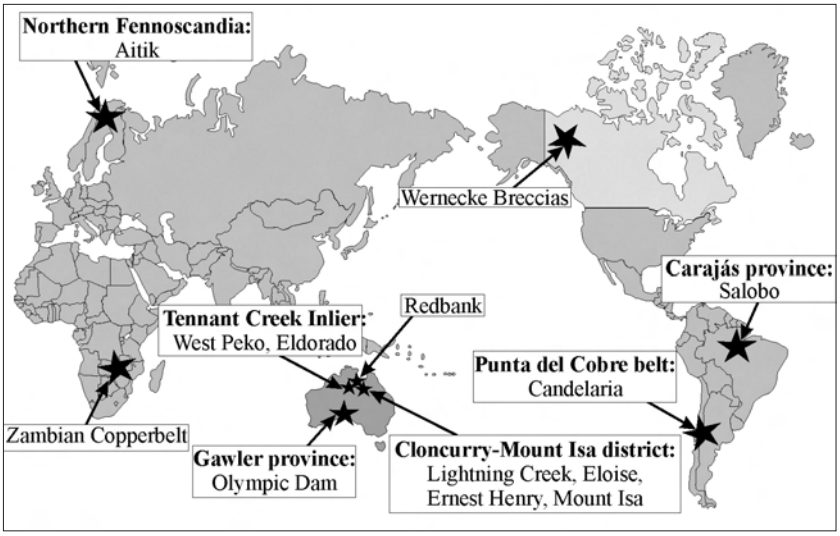

Fig. 1. Location of selected IOCG districts. Also shown are the locations of sediment-hosted copper deposits in the Mount Isa region and the Zambian copper belt. Modified from Hitzman (2000).

The IOCG end of the spectrum is loosely defined, and globally incorporates copper (± gold ± uranium) deposits of Archean to Tertiary age that are linked primarily by the presence of abundant Ti-poor (<2 wt.% TiO_2) magnetite and/or hematite, and extensive alteration, particularly Fe-, Na-, and K-metasomatism (Hitzman et al., 1992; Hitzman, 2000; Sillitoe, 2003; Williams et al., 2005a). However, there are also noteworthy differences, both between deposits within a district and between districts, and this has led to a number of contrasting genetic models. Some authors propose formation from dominantly magmatic fluids (e.g., Hitzman et al., 1992; Pollard et al., 1998; Wyborn, 1998; Skirrow, 1999; Perring et al., 2000; Pollard, 2000, 2001). Others propose magmatic fluid as the main source of metals (and sulfur), but invoke mixing with different fluids, usually cooler, less saline and more oxidizing, as the mechanism responsible for metal precipitation (e.g., Reeve et al., 1990; Baker, 1998; Mark et al., 2000; Marschik and Fontboté, 2001); the contribution made to the metal budget by these additional fluids is not clear. Several authors suggest non-magmatic fluids are necessary for the formation of IOCG mineralization (e.g., Haynes et al., 1995; Barton and Johnson, 1996, 2000; Haynes, 2000; Hitzman, 2000) and that magmatism is important primarily as a source of heat to drive hydrothermal convection (Barton and Johnson, 1996, 2000).

New information from Wernecke Breccia-associated IOCG prospects suggests the above spectrum of magmatic and hybrid magmatic–non-magmatic models for IOCG deposits should be expanded to accommodate IOCG systems formed in an environment unrelated to magmatism: those formed from non-magmatic fluids circulated by non-magmatic processes.

To reflect this variability, modifications to the definition of IOCG systems are proposed that accommodate the degree of involvement of magmatic and/or non-magmatic fluids and the nature of the mineralizing environment. This division expands on distinctions made between iron oxide-rich systems by earlier authors (e.g., Barton and Johnson, 2000; Barton et al., 2000; Williams et al., 2005a), and enables the characteristics of individual IOCG types to be better delineated, thus providing more narrowly defined attributes to be used in mineral exploration models. It is suggested that IOCG systems be divided into non-magmatic end members (i.e., those formed by non-magmatic fluids in an amagmatic environment), and magmatic end members. Magmatic end members are closely associated in time and space with igneous intrusions and their magmatic fluids (but excluding magnetite-apatite Kiruna-type deposits as suggested by Hitzman, 2000). Hybrid IOCG systems, formed from a combination of magmatic and non-magmatic hydrothermal fluids, would fall in between the two end members. The characteristics of end-member and hybrid IOCG systems are presented along with brief descriptions of example deposits, including a summary of new information for Wernecke Breccia-related deposits.

The range of IOCG systems may form a link between intrusive- and sedimentary-related deposits. IOCG systems dominated by magmatic and magmatic–non-magmatic fluids have been compared to porphyry deposits (e.g., Barton and Johnson, 2000; Pollard, 2000; Sillitoe, 2003) and the two deposit types are considered to form a continuum of intrusion-related deposits (e.g., Pollard, 2000; Sillitoe, 2003). IOCG systems dominated by highly saline non-magmatic fluids have similarities to some sediment-hosted Cu deposits, for example, Mount Isa and the Zambian copper belt. Thus, information gained from IOCG deposits is not unique to the deposit type, but can also be used in the study of, and in exploration for, other types of mineral deposits.

Table 1. Size and Grade of Selected IOCG Deposits

Deposit	Tonnes (× 10^6)	Commodity	Grade	Associated Metals	Mineralization Styles
Magmatic End-Member IOCG					
Lightning Creek[1]	–	Cu (%) Au (g/t)	minor minor	–	Qz-Mt ± Py ± chalcopyrite veins
Eloise[2]	3.2	Cu (%) Au (g/t) Ag (g/t)	5.8 1.5 19	Co, Ni, Zn, As, Bi	Veins, stockwork veins, massive sulfide
Hybrid Magmatic–Non-Magmatic IOCG					
Olympic Dam[3]	2320	Cu (%) Au (g/t) Ag (g/t) U_3O_8 (kg/t)	1.3 0.5 2.9 0.4	Co, REE (dominantly La and Ce), Ni, As	Disseminations, veinlets, and fragments within breccia zones, primarily within breccia matrix
Aitik[4]	800	Cu (%) Au (g/t) Ag (g/t)	0.3 0.2 2	Mo	Disseminations and veins
Candelaria[5]	470	Cu (%) Au (g/t) Ag (g/t)	.95 .22 3.1	Zn, Mo, As, LREE	Vein, breccia-hosted, mantos, overprints Mt replacement bodies
Salobo[6]	450	Cu (%) Au (g/t)	1.15 0.5	Ag, U, Co, Mo, F, LREE	Lenses, veins
Ernest Henry[7]	166	Cu (%) Au (g/t)	1.1 0.54	Co, Mo, U, REE, F, Mn, As, Ba	In breccia
Non-Magmatic End-Member IOCG					
Wernecke Breccia[8]	Slab: 20	Cu (%)	0.35	U, Co, Mo	Disseminations, veins, breccia infill
Tennant Creek[9]	West Peko: 3.2 Eldorado: 0.0292	Cu (%) Au (g/t)	4 20.8	Bi	Massive and vein mineralization overprinting ironstone
Redbank[10]	Bluff: 2 Sandy Flat: 1.5	Cu (%) Cu (5)	1.66 2	Pb, Zn, REE	Breccia infill, veins, disseminations

Note

[1]Perring et al. (2000), Williams et al. (1999).

[2]Baker (1998), Baker and Laing (1998), Baker et al. (2001).

[3]Roberts and Hudson (1983, 1984), Creaser (1989), Reeve et al. (1990), Johnson and Cross (1991), Oreskes and Einaudi (1992), Oreskes and Hitzman (1993), Eldridge (1994), Haynes et al. (1995), Reynolds (2000).

[4]Frietsch et al. (1995, 1997), Carlon (2000), Wanhainen et al. (2003).

[5]Ullrich and Clark (1999), Marschik and Fontboté (1996, 2001), Marschik et al. (2000).

[6]Requia and Fontboté (2000), Souza and Vieira (2000).

[7]Twyerould (1997), Ryan (1998), Mark and Crookes (1999), Mark et al. (2000), Williams et al. (unpub.data, 2006).

[8]Hunt et al. (2004, 2005).

[9]Ahmad et al. (1999), Skirrow and Walshe (2002).

[10]Orridge and Mason (1975), Knutson et al. (1979).

Abbreviations: Mt = magnetite, Py = pyrite, Qz = quartz.

IOCG Systems

End-Member Non-Magmatic IOCG Systems

New geological, fluid inclusion, and stable isotope data indicate IOCG mineralization associated with Wernecke Breccia formed from highly saline non-magmatic fluid (Hunt, 2005; Hunt et al., Hunt et al., unpub. data, 2006). Other possible non-magmatic end-member systems include deposits in the Tennant Creek inlier and Redbank areas of the Northern Territory of Australia (Fig. 1).

Wernecke Breccia: Iron oxide Cu (± Au ± U) mineralization associated with Wernecke Breccia is found in areas of the north-central Yukon Territory that are underlain by the Paleoproterozoic Wernecke Supergroup (WSG; Figs. 2, 3; Table 2). The WSG is an approximately 13 km-thick package of marine fine-grained sandstone, siltstone, dolostone, and minor limestone (e.g., Gabrielse, 1967; Delaney, 1981; Bell, 1986a,b; Thorkelson, 2000) that was metamorphosed to greenschist facies and multiply deformed during the Proterozoic Racklan orogeny (e.g., Thorkelson, 2000; Brideau et al., 2002). Bodies of ca. 1595 Ma-old (Thorkelson, 2000; Thorkelson et al., 2001a) Wernecke Breccia crosscut the WSG and are made up largely of clasts of the supergroup in a matrix of rock flour and hydrothermal precipitates (Fig. 3a). At least 65 bodies of Wernecke Breccia are known and all are associated with iron oxide-Cu (± Au ± U ± Co) mineralization, including the Slab (Table 1), Hoover, Slats, Igor, and Olympic prospects that were examined in this study (Figs. 2, 3). Mineralization occurs as disseminations and veins within Wernecke Breccia and surrounding WSG rocks, and is largely made up of early magnetite and/or hematite and later chalcopyrite and pyrite (Fig. 4b,c; e.g., Brookes et al., 2002; Hunt et al., 2002, 2005; Thorkelson et al., 2003; Yukon MINFILE, 2007). Gold-bearing phases were not observed, but gold reports with copper in assay results (e.g., Yukon MINFILE, 2007). Uranium (pitchblende, brannerite) and minor cobalt (cobaltian pyrite, erythrite) mineralization occurs locally. Gangue is dominantly composed of carbonate (calcite, dolomite, siderite), quartz, albite, and K feldspar, with lesser biotite, muscovite, chlorite, and fluorite; minor rutile, epidote (some is allanite), apatite, tourmaline, and monazite occur locally (e.g., Brookes et al., 2002; Hunt et al., 2002, 2005). Extensive sodic or potassic metasomatic alteration is spatially associated with the breccia bodies, and they are cut by late-stage carbonate veins dominantly composed of calcite and/or dolomite/ankerite that contain minor pyrite and chalcopyrite and trace molybdenite (Table 3; Hunt et al., 2002, 2005). At the Igor prospect, late-stage veins are com-

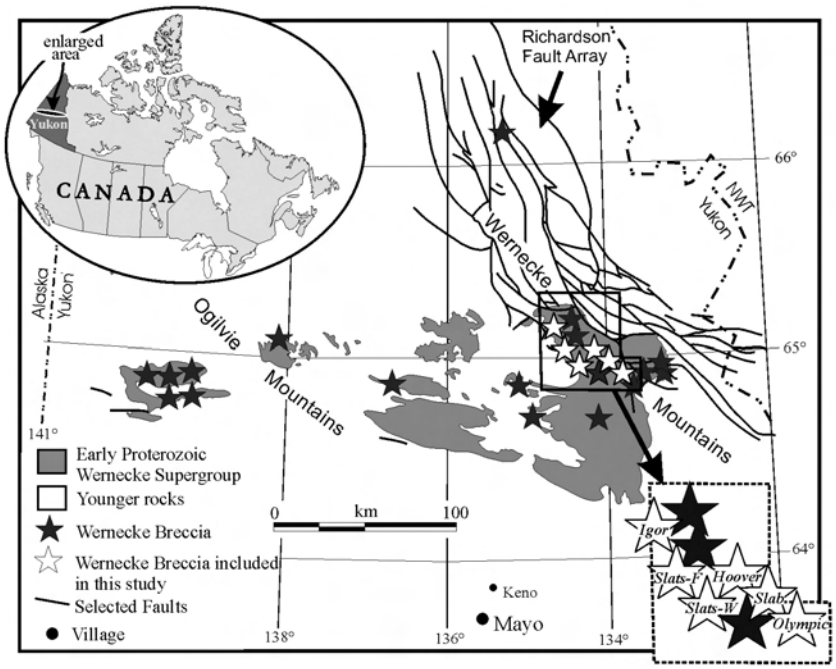

Fig. 2. Distribution of Wernecke Breccia and location of breccia-associated IOCG prospects included in this study (modified from Thorkelson, 2000).

posed dominantly of barite ± siderite.

The breccia bodies are associated with faults on a regional scale (Richardson Fault array) as well as at local scale (Figs. 2, 3; e.g., Bell and Delaney, 1977; Bell, 1978, 1986a,b; Thorkelson, 2000). They formed in weak zones such as faults and shear zones, fold axes, and lithological contacts possibly by fluid-driven failure (e.g., Cox and Ruming, 2004) when permeability seals were breached. Crosscutting relationships indicate multiple phases of brecciation and mineralization occurred syn- to post-deformation but after peak metamorphism (e.g., Thorkelson, 2000; Brideau et al., 2002; Hunt et al., 2005). Wernecke Breccia occurs throughout the WSG, but is most abundant in the lower part of the stratigraphy (Delaney, 1981; Lane, 1990), where there is a transition from calcareous sedimentary strata that contain halite facies meta-evaporites to

Table 2. Synopsis of Tectonic Setting, Main Host Rocks, Confining Structure, and Age of Mineralization for Selected IOCG Deposits

Deposit	Tectonic Setting	Main Host Rocks	Confining Structure	Age of Mineralization (Ma)	Coeval Intrusions
		Magmatic End-Member IOCG			
Lightning Creek	Intracratonic basin associated with high heat flow and plutonism	ca. 1540–1500 intrusive rocks	–	Coeval with late-stage sills	Yes
Eloise		Meta-arkose, schist, amphibolite of the Soldiers Cap Group (ca. 1670–1600 Ma)	Shear zones	ca. 1536–1512 (Ar-Ar, biotite, hornblende)	Inferred
		Hybrid Magmatic–Non-Magmatic IOCG			
Olympic Dam	Anorogenic intracontinental environment above a mantle plume; or arc–back-arc	Granite and felsic, mafic, and ultramafic volcanic rocks of the ca. 1590 Ma Hiltaba Suite/Gawler Range volcanics	Dilational zone in regional-scale fault	ca. 1590	Yes
Aitik	Volcanic arc–back arc basin above a subduction zone	ca. 1910–1880 Ma intermediate to felsic metavolcanic rocks	Fault/shear zones	ca. 1870	Yes
Candelaria	Arc–back-arc	Early Cretaceous intrusive, volcanic, volcaniclastic and sedimentary rocks	Intersection of shear zone and faults with lithologic contact		
Salobo	Continental rift	Metagreywacke and amphibolite of the ca. 2750 Ma Itacaiúnas Super Group	Shear zone		
Ernest Henry	Intracratonic basin associated with high heat flow and plutonism	Brecciated, altered, intermediate to felsic ca. 1740 Ma volcanic rocks (ca. 1780–1720? Ma)	Shear zones		
		Non-Magmatic End-Member IOCG			
Wernecke Breccia	Rifted continent?	> ca. 1710 Ma meta-sandstone, siltstone, dolostone, limestone, and evaporites of the Wernecke Supergroup	Shear zones, faults, fold axes		
Tennant Creek	Pull-apart sedimentary basin	ca. 1680 Ma Warramunga Formation	Inronstone in shear zones and fold axes		
Redbank	Rifted continent	Middle Proterozoic Tawallah Group, in part ca. 1575 ± 120 Ma	Faults		

Note
References as in Table 1.

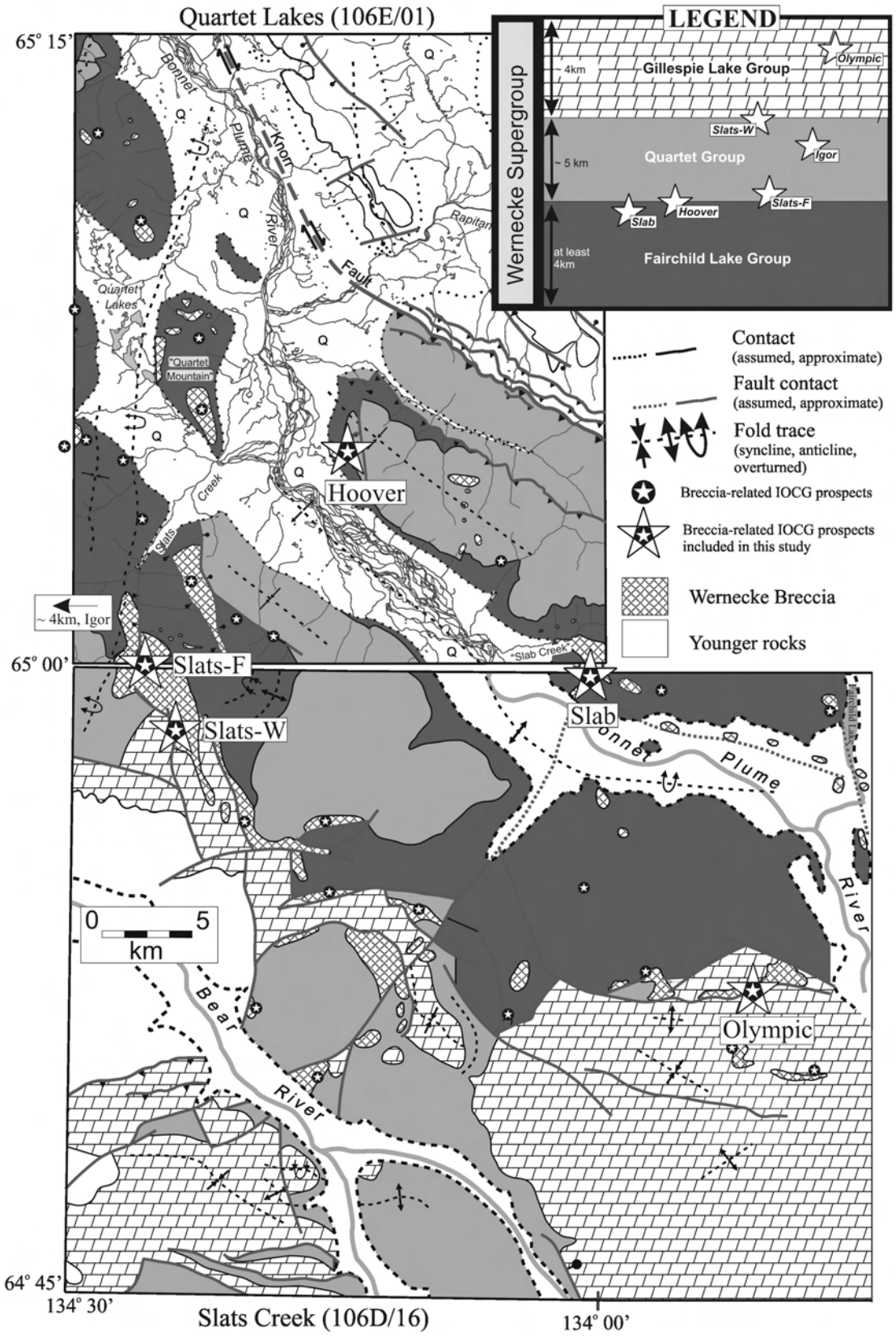

Fig. 3. Simplified bedrock geology map of the study area (for details see Thorkelson, 2000; Thorkelson et al., 2002, 2003). Legend shows approximate stratigraphic position of IOCG prospects studied.

overlying, locally pyritic, carbonaceous shale (Hunt et al., 2005). Fluid pressure calculated from fluid inclusion data for breccias at this stratigraphic level ranges from approximately 2.5 to 3 kb, indicating a depth of emplacement of about 7.5 to 9.0 km, roughly equivalent to the thickness of overlying WSG strata (Hunt, 2005; Hunt et al., unpub. data, 2006).

All Wernecke Breccia prospects examined in this study are spatially associated with volumetrically minor Bonnet Plume River intrusions. These intrusions are mafic to intermediate in composition and generally form narrow (<1–5 m wide) dikes and sills, and small stocks throughout the study area (Thorkelson, 2000; Thorkelson et al., 2001b). The intrusive rocks occur as clasts in Wernecke Breccia and are thus clearly older than the breccia bodies. U-Pb (zircon) dating of four Bonnet Plume River intrusions shows they are ca. 1710 Ma old (Thorkelson et al., 2001b), which precludes a genetic link between Bonnet Plume River magmatism and breccia/mineralizing fluids (1710 Ma vs. 1595 Ma). The spatial coincidence of Wernecke Breccia and Bonnet Plume River intrusions appears to be a consequence of the use of the same fluid pathways. Similarly, ca. 1270 Ma dikes of the Bear River suite also occur in these sites, indicating that these fluid pathways were important for hundreds of millions of years. In addition, ductility contrasts between Bonnet Plume River intrusions and host WSG sedimentary rocks may have produced dilational zones during folding, which focused hydrothermal fluid flow and led to preferential development of breccia in these sites.

Clasts of mafic to intermediate volcanic rocks, known as the Slab volcanics, have also been recognised locally within Wernecke Breccia (Thorkelson, 2000; Thorkelson et al., 2001a; Laughton, 2004; Laughton et al., 2005). Attempts

Table 3. Regional and Ore-related Alteration Types for Selected IOCG Deposits

Deposit	Regional Alteration	Dominant IOCG-Related Mineralization		
		Early	Main	Late
		Magmatic End-Member IOCG		
Lightning Creek	Sodic-calcic	Ca-Fe ± Na	Pyroxene-albite ± magnetite; quartz-magnetite ± clinopyroxene ± albite ± pyrite. Dominant ore mineral: chalcopyrite	Ca ± Cl
Eloise	Pervasive albitization	Hornblende, biotite, quartz veins and alteration ± albite	Quartz, calcite, actinolite/hornblende, chlorite, biotite, muscovite, K feldspar. Dominant ore mineral: chalcopyrite	Chlorite, K feldspar, siderite-hematite, calcite veins; silicification and chlorite-calcite veins; pyrite-quartz-adularia veins
		Hybrid Magmatic–Non-Magmatic IOCG		
Olympic Dam	Weak pervasive hematite, sericite, and chlorite.	Magnetite ± hematite, chlorite, sericite, siderite	Intense hematite and chlorite is associated with mineralization in the lower part of the deposit; sericite and silica predominates in the upper part. Dominant ore minerals: chalcocite, bornite, chalcopyrite, uraninite	Hematite ± quartz ± barite
Aitik	Scapolite, albite ± tourmaline	–	Biotite and sericite in the ore zone; K feldspar and epidote in fault zones. Dominant ore minerals: chalcopyrite, bornite ± chalcocite	Sericite/muscovite
Candelaria	Pervasive albitization	Biotite-quartz-magnetite ± K feldspar	Calcic amphibole-albite ± K feldspar. Dominant ore minerals: chalcopyrite; locally abundant sphalerite	Epidote-chlorite; hematite-calcite-chalcopyrite; anhydrite and calcite-chlorite
Salobo	Na, K	Magnetite, hematite	K feldspar, biotite. Dominant ore minerals: chalcopyrite, bornite, chalcocite	Calcic; chlorite
Ernest Henry	Na–Ca	Disseminated biotite-magnetite; garnet-K feldspar-biotite	K feldspar-hematite. Dominant ore minerals: chalcopyrite, chalcocite	Dominantly calcite-dolomite; minor quartz-biotite-actinolite-pyrite-magnetite-± garnet ± chalcopyrite veins and breccia
		Non-Magmatic End-Member IOCG		
Wernecke Breccia	Greenschist facies metamorphism	Sodic ± potassic; potassic ± sodic; local pervasive biotite; local magnetite-ankerite	Sodic ± potassic; potassic ± sodic; carbonate; local sericite. Dominant ore mineral: chalcopyrite	Calcite or dolomite-ankerite or barite ± siderite ± ankerite-dolomite; local overprinting chlorite-magnetite
Tennant Creek	Weakly metamorphosed	Magnetite-hematite-quartz ± chlorite ironstone	Chlorite ± stilpnomelane ± talc ± siderite ± calcite (reduced end member); chlorite-sericite-hematite (oxidized end member). Ore minerals include: chalcopyrite, bismuthinite and gold	–
Redbank	Pervasive K	Chlorite-hematite-K feldspar	Chlorite-hematite-K feldspar	–

Note

References as in Table 1.

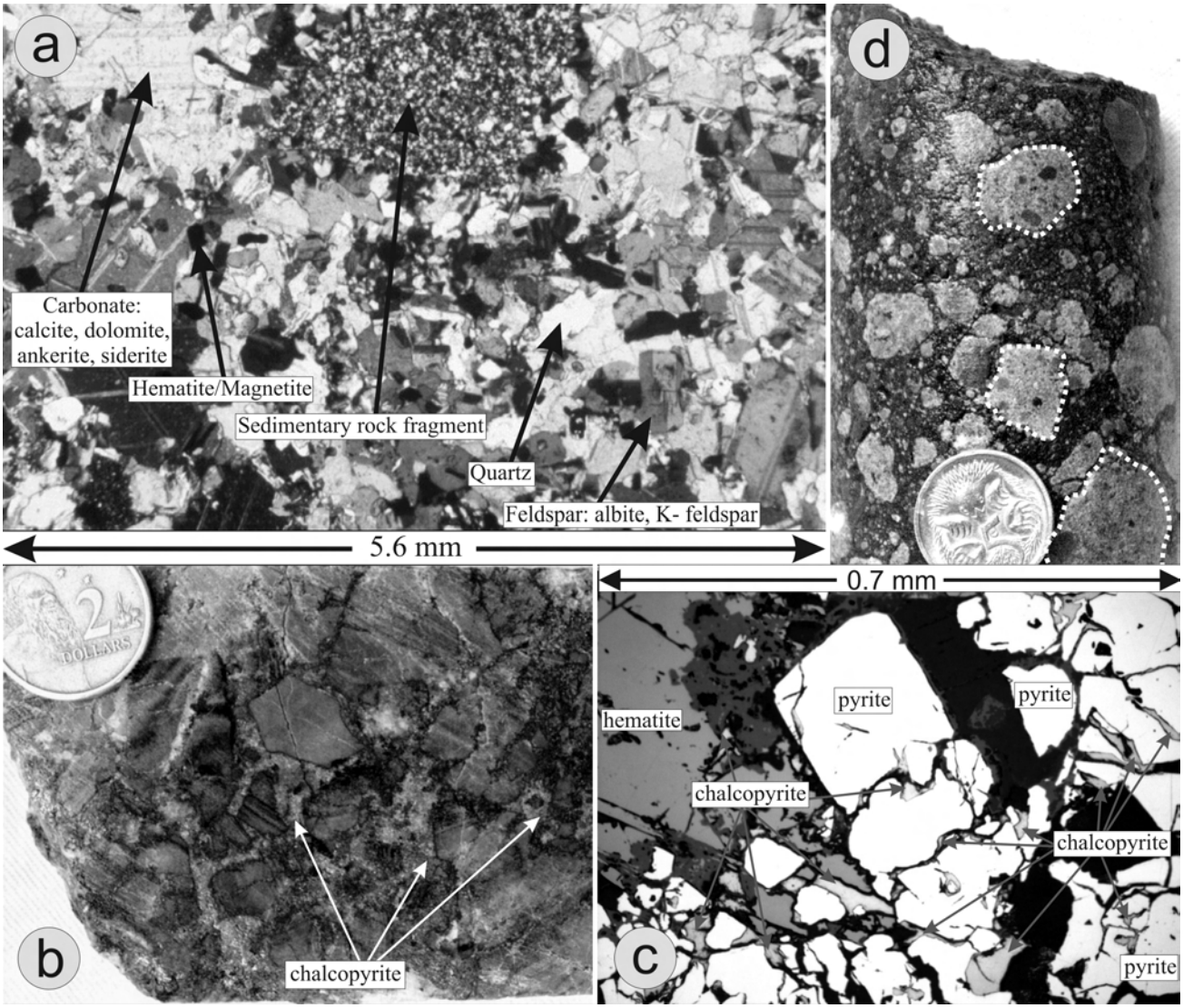

Fig. 4. Typical examples of Wernecke Breccia and associated IOCG mineralization and alteration: ***a.*** Photomicrograph of Wernecke Breccia matrix (transmitted cross-polarized light) made up dominantly of sedimentary rock fragments, carbonate, feldspar, lesser quartz, and minor hematite and magnetite; ***b.*** Chalcopyrite-forming matrix to breccia, Hoover prospect; ***c.*** Photomicrograph of hematite overgrown by pyrite with chalcopyrite filling fractures (plane-polarized reflected light), Olympic prospect; ***d.*** Breccia with abundant clasts of earlier breccia, Slab area.

at dating the Slab volcanic rocks have been unsuccessful and their age remains poorly constrained. Crosscutting relationships show they are older than Wernecke Breccia, but the difference in age between the timing of breccia emplacement and volcanism is unknown. However, Slab volcanic rocks have been observed only locally, and thus are unlikely to have been responsible for the brecciation that is observed over distances of hundreds of kilometers.

Fluids that formed Wernecke Breccia and the associated mineralization were moderate temperature (185°–350°C), high salinity (24–42 wt.% NaCl eq.) NaCl–$CaCl_2$ brines (Fig. 5; Table 4; Hunt et al., 2004; Hunt, 2005; Hunt et al., unpub. data, 2006). Carbon and oxygen isotopic compositions for hydrothermal carbonates at the prospects studied range from $\delta^{13}C_{carbonate}$ = –7 to +1‰ (V-PDB) and $\delta^{18}O_{carbonate}$ = –2 to +20‰ (V-SMOW). Calculated $\delta^{18}O_{fluid}$ values derived from carbonate range from approximately –8 to +14‰ (Fig. 6). Sulfur isotope values for hydrothermal pyrite, chalcopyrite and barite range from $\delta^{34}S_{pyrite/chalcopyrite}$ = –13 to +14‰ (CDT) and $\delta^{34}S_{barite}$ = 7 to 18‰ (CDT; Fig. 6). The $\delta^{18}O$ values for hydrothermal carbonates generally reflect those of the host WSG strata and $\delta^{13}C$ values indicate that carbon was derived in large part from the WSG. The $\delta^{34}S$ values of pyrite, chalcopyrite, and barite point to seawater (or sediments/evaporites deposited from seawater) as a likely source for much of the sulfur, with possible additional sulfur from the leaching of biogenic pyrite and/or sulfides in local igneous rocks. The carbon, oxygen, and sulfur isotopic compositions combined with limited hydrogen isotope data indicate that fluids were likely derived from formation/metamorphic water mixed with variable amounts of low-δD water (e.g., organic

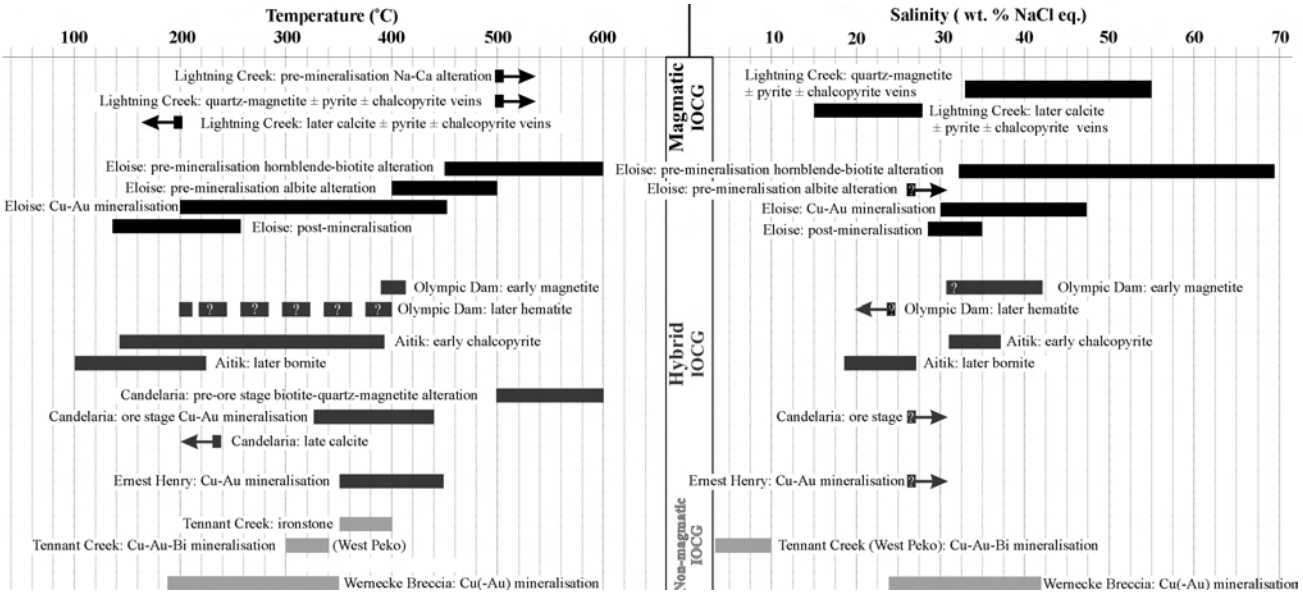

Fig. 5. Fluid temperature and salinity data for selected IOCG deposits and prospects. References as in Table 1.

water) ± evolved meteoric and/or evolved seawater. The high salinity of the fluid is consistent with derivation from an evaporite-bearing sedimentary sequence (e.g., Yardley and Graham, 2002). Magmatic waters are considered less likely as a fluid source because there are no igneous rocks of appropriate age and distribution. Fluids sourced from buried intrusions and/or high-temperature volcanic vapors are geologically feasible; however, the available fluid inclusion and stable isotopic data do not clearly indicate the input of abundant magmatic fluid.

The lack of an obvious intrusive heat source suggests that fluid circulation and the high temperatures reached by the fluid(s) occurred via mechanisms other than those related to magmatic heat flow. Temperatures would have increased within the basin during emplacement of the Bonnet Plume River intrusions and throughout prograde metamorphism. The presence of marialitic scapolite in metahalite layers in the lower part of the WSG indicates that temperatures reached at least 400°C (e.g., Kwak, 1977) in the deep part of the basin during metamorphism. However, peak metamorphism occurred prior to brecciation, and metamorphic/basinal fluids may have cooled considerably before breccia emplacement and mineralization occurred. Nevertheless, fluid temperatures in at least the deeper part of the WSG would have been elevated due to the thickness of overlying sediments. A simple burial model would produce fluids with the required high temperatures. An average geothermal gradient of 25° to 30°C (e.g., Raymond, 1995, 2000) and a surface temperature of 25°C would produce temperatures of 250° to 295°C at depths of 7 to 9 km. The geothermal gradient may have been higher than average in the Wernecke Mountains area because it is postulated to have been a rifting/extensional environment during deposition of the WSG and emplacement of the Bonnet Plume River intrusions (Thorkelson, 2000; Thorkelson et al., 2001b). Crosscutting relationships indicate Wernecke Breccias were formed syn- to post-deformation (Thorkelson, 2000; Hunt et al., 2005); thus, fluid circulation could have been driven by tectonic (and/or gravity) processes (e.g., Torgersen, 1990; Garven et al., 2001). Another possible mechanism to provide high-temperature fluids and to drive circulation is the method proposed by Deming (1992), whereby heat is released periodically from the continental crust by the onset of free convection in orogenic zones. With this mechanism, deformation increases the permeability of the crust and causes deep, transitory circulation of fluids through the upper crust, setting up free convection cells. The free convection cells periodically supply a tectonically/gravity-driven flow system with heat (and possibly metals) as they form, release heat from the crust, and then die out. Thus, the influx of heat is transitory, but may be large.

The source of metals that formed IOCG mineralization associated with Wernecke Breccia is unknown, but may have been the host strata. Analyses of reportedly unmineralised samples of WSG (Goodfellow, 1979; Lane, 1990; Thorkelson, 2000) indicate that the Fairchild Lake and Quartet groups contain elevated levels of Cu (up to 1230 ppm), U (up to 40 ppm), and Co (up to 27 ppm), and thus could have acted as a source of metals. Bonnet Plume River intrusions and Slab volcanic rocks locally contain disseminated chalcopyrite and/or malachite, and could have acted as sources of copper. Published geochemical analyses indicate Cu contents of up to 2124 ppm and 11.6 ppm, respectively, for the Bonnet Plume River intrusions and Slab volcanic rocks (Thorkelson, 2000); however, the samples were collected proximal to Wernecke Breccia and the results may therefore not represent background values.

Tennant Creek: Iron oxide-associated Au-(Cu-Bi) deposits in the Tennant Creek area, Australia (e.g., West Peko and Eldorado; Table 1), are hosted by ca. 1860 Ma (Compston, 1995) weakly metamorphosed greywacke, siltstone, and

Table 4. Fluid Temperature, Salinity, Composition, and Source, Plus Precipitation Mechanisms for Selected IOCG Deposits

Deposit	Phase	Temperature (°C)	Salinity (wt.% NaCl eq.)	Fluid Source	Precipitation Mechanism
		Magmatic End-Member IOCG			
Lightning Creek	Na–Ca alteration	>500	–	Magmatic	Decrease in temperature and salinity, fluid mixing
	Quartz-magnetite ± pyrite ± chalcopyrite veins	>500	33–55	Magmatic	
	Later calcite ± chlorite ± pyrite ± chalcopyrite veins	<200	15–28	Magmatic + meteoric?	
Eloise	Pre-mineralization hornblende-biotite alteration	450–600	32–68	Magmatic?	Decrease in temperature and salinity, increase in pH, and dilution due to fluid mixing; sulfidation of Fe-silicates
	Pre-mineralization albite alteration	400–500	>26	Magmatic?	
	Mineralization	200–450	30–47	Magmatic?	
	Post-mineralization	137–258	29–35	Magmatic? mixed with meteoric	
		Hybrid Magmatic–Non-Magmatic IOCG			
Olympic Dam	Early magnetite	~400	31?–42	Magmatic or deeply circulating water	Fluid mixing; superimposed hot and cooler fluids; cooling
	Ore formation (hematite)	200–400	<24	Surficial/connate	
	Fluorite-quartz with bornite-chalcocite	Th = avg 240	–	–	
	Fluorite-quartz with chalcopyrite	Th = avg 160	–	–	
Aitik	Chalcopyrite	140–373	31 –37	Magmatic ± evaporitic	Fluid mixing?
	Bornite	100–222	18–27		
Candelaria	Biotite-quartz-magnetite alteration	500–600	–		Cooling ± fluid mixing
	Cu-Au	330–440	>26	Magmatic ± non-magmatic	
	Late calcite	≤236	–		
Salobo	–	–	–	Magmatic + connate + more oxidized fluid	Fluid mixing
Ernest Henry	Ore fluid	350–450	>26	Magmatic + ?	Fluid mixing and/or cooling
		Non-Magmatic End-Member IOCG			
Wernecke Breccia	Ore fluid	185–350	24–42	Formation/metamorphic water	Cooling?, fluid mixing?
Tennant Creek	West Peko: Ore fluid	300–340	3–10 (low)	Metamorphic/formation water	Reaction of reducing fluid with ironstone
	Eldorado: Ore fluid	~300	Low to moderate	Metamorphic/formation water +?	Fluid mixing in presence of ironstone
Redbank	Carbonate	–	–	Formation water ± seawater	Decrease in temperature

Note
References as in Table 1.

shale of the Warramunga Formation (Table 2; Large, 1975; Skirrow and Walshe, 2002). The deposits appear to be structurally controlled and overprint older ironstone bodies (Wedekind and Love, 1990; Huston et al., 1993; Skirrow and Walshe, 2002). For example, West Peko is located proximal to the axis of a regional-scale syncline, and the chalcopyrite-gold-bismuthinite mineralization overprints the central parts of two magnetite-hematite-quartz-chlorite ironstone bodies (Table 3). The Eldorado Au-Bi deposit occurs within parasitic folds on the limb of a regional-scale anticline, and mineralization occurs mainly in stringer and breccia zones that broadly correlate with areas of pervasive silicification and zones of higher magnetite-(hematite-martite) abundance located near a change in the trend of the ironstones.

The ironstone bodies formed from hot (350°–400°C) NaCl + $CaCl_2$ brines (probably formation waters) at pressures of approximately 2.5 to 5 kb (Fig. 5; Wedekind and Love, 1990; Skirrow and Walshe, 2002). Gold-Cu-Bi mineralization at the West Peko deposit is interpreted to have formed from pyrrhotite ± magnetite-stable, 300° to 340°C, weakly acidic, sulfur- and N_2±CH_4-rich, low salinity (3–10 wt.% NaCl eq.) hybrid metamorphic–formation waters

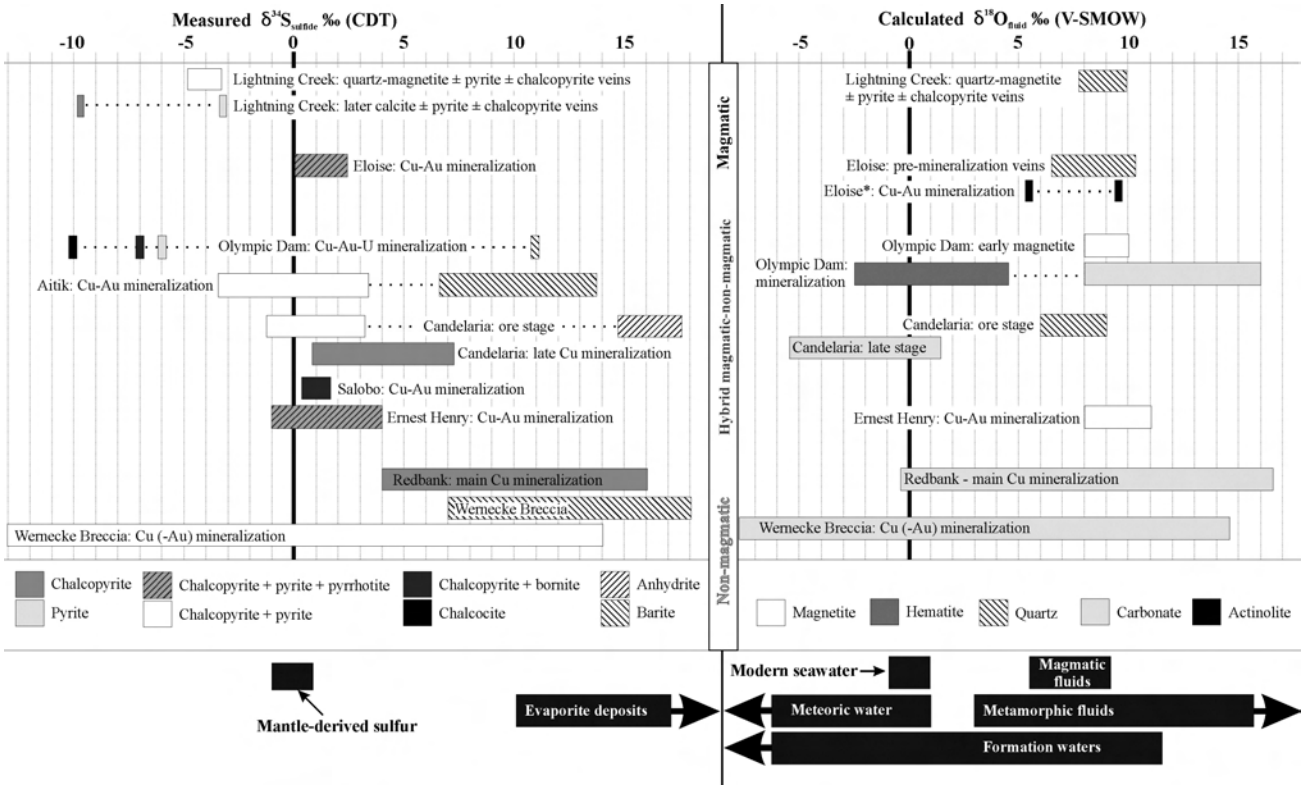

Fig. 6. Measured sulfur isotope compositions for mineralization and calculated oxygen isotope compositions for mineralizing fluid from selected IOCG deposits. Legend shows mineral(s) used for sulfur isotope analysis and mineral used to calculated oxygen isotopic composition of fluid. References as in Table 1. Lower part of diagram shows $\delta^{18}O$ values for magmatic, metamorphic, formation, and meteoric waters and modern seawater (e.g., Sheppard, 1986; Rollinson, 1993) plus $\delta^{34}S$ values for mantle and evaporite sulfur sources (e.g., Ohmoto and Goldhaber, 1997).

(Fig. 5; Table 4; Skirrow and Walshe, 2002). This fluid likely flowed along shear and fault zones, which tapped reduced rock packages beneath the oxidized Warramunga Formation. Gold and native bismuth were deposited in response to desulfidation ± oxidation of the reduced fluid as it reacted with magnetite ± hematite-rich ironstone. Desulfidation may have been driven by precipitation of chalcopyrite, pyrite, pyrrhotite, and Bi-sulfides or sulfosalts in response to increased pH of the fluids (Skirrow, 1999; Skirrow and Walshe, 2002). Eldorado mineralization is interpreted to have formed from intermediate f_{O_2}, low- to moderate-salinity ore fluid (a variant of the reduced fluid that formed West Peko mineralization), which mixed with hematite-stable Ca-Na-Cl brine in the presence of magnetite-rich ironstone (Skirrow and Walshe, 2002). Fluid mixing likely caused an increase in Cu solubility leading to undersaturation of Cu minerals and the deposition of Au-Bi mineralization without Cu phases.

The mechanism of fluid circulation and the source of heat and metals for the Tennant Creek deposits are not clear (Large, 1975; Wedekind and Love, 1990; Skirrow and Walshe, 2002). The West Peko deposit occurs several hundred meters above a 300 to 500 m-thick stratiform quartz-potassium feldspar-plagioclase porphyry, and geophysical data for the Eldorado area indicate that granite occurs nearby (Skirrow and Walshe, 2002). However, the age of the intrusive rocks is not well constrained, and hence their role as a potential heat or metal source is not known. The deposits are associated with regional-scale structures and Au-(Cu-Bi) mineralization occurred during deformation (Wedekind and Love, 1990; Skirrow and Walshe, 2002), suggesting that fluid flow may have been related to tectonic processes, or may have been topographically driven. Metals may have been derived from the host sedimentary strata and/or igneous rocks as fluid flowed along shear and fault zones.

Redbank: IOCG prospects in the Redbank area, Australia (Fig. 1), are hosted by sedimentary and volcanic rocks of the Paleoproterozoic Tawallah Group (<1780–1720 Ma) in the McArthur Basin (Knutson et al., 1979; Jackson and Southgate, 2000; Betts et al., 2003). Approximately 50 breccia pipes are located along a series of basement faults (Orridge and Mason, 1975; Knutson et al., 1979). Brecciation, was accompanied by pervasive potassium and iron metasomatism and is reflected by the presence of abundant K feldspar, hematite, and chlorite in breccias and host strata (Knutson et al., 1979). Several of the pipes contain significant copper mineralization, for example, Bluff and Sandy Flat, where chalcopyrite and minor covellite and chalcocite occur as breccia infill and as veins and disseminations in breccia clasts and host rocks (Table 1; Knutson et al., 1979).

Sulfur isotopic compositions for the main copper min-

eralization range from $\delta^{34}S \approx 4‰$ to 16‰; carbon and oxygen isotopic values for hydrothermal dolomite associated with this mineralization range from $\delta^{13}C = –4.6‰$ to +3.2‰, and $\delta^{18}O = 13.1‰$ to 22.6‰ (Knutsen et al., 1979). Knutsen et al. (1979) suggested that the wide range of positive sulfur isotopic compositions and the carbon and oxygen isotopic values, which range up to those typical of unaltered dolostone in this region, indicate deposition from heated connate brines and/or marine waters rather than magmatic-hydrothermal fluids. However, deeper parts of the stratigraphy in this region do contain minor amounts of sulfide ($\delta^{34}S = –2.0‰$ to –1.3‰) and carbonate mineralization that are interpreted to be of magmatic hydrothermal origin. Fluids that formed the main copper mineralization may have circulated through this material and leached S, C, and metals that were subsequently re-deposited within the breccia pipes higher in the stratigraphy, thus giving the observed wide range of isotopic values.

End-member Magmatic IOCG Systems

IOCG deposits at the magmatic end of the spectrum formed from ore fluids with a dominantly magmatic origin and are typified by deposits such as Lightning Creek and Eloise, Australia (Tables 1–4; Fig. 1). The deposits are generally spatially and/or temporally associated with igneous rocks (e.g., Lightning Creek; Perring et al., 2000). Exposed, coeval igneous rocks are not always present, but the presence of buried intrusions may be inferred from geophysical data (e.g., Eloise; Baker, 1998). Fluid was moderate to high temperature and saline (Fig. 5; Table 4), and circulated by heat from magmatism (e.g., Adshead et al., 1998; Pollard, 2000, 2001). Isotopic values indicate that sulfur and fluids were derived from a magmatic source (Fig 6).

Lightning Creek and Eloise: The Lightning Creek and Eloise deposits are located in the Cloncurry district of Australia in the eastern part of the Mount Isa inlier, and are hosted by sedimentary and volcanic rocks that have been divided into three superbasin sequences: Leichhardt (ca. 1800–1750 Ma), Calvert (ca. 1730–1690 Ma), and Isa (ca. 1670–1575 Ma; Fig. 1; Table 2; Beardsmore et al., 1988; Blake and Stewart, 1992; Adshead et al., 1998; Scott et al., 2000; Southgate et al., 2000; Williams and Skirrow, 2000). Deformation and metamorphism of the host rocks occurred during the Diamantina (ca. 1600 Ma) and Isan orogenies (ca. 1550–1500 Ma; O'Dea et al., 1997; Betts et al., 1998; Laing, 1998; MacCready et al., 1998), and significant granitoid igneous activity occurred ca. 1550 Ma and ca. 1540 to 1500 Ma (Page and Sun, 1998; Pollard et al., 1998; Wyborn, 1998). Intense, widespread sodic-calcic alteration is temporally and spatially associated with emplacement of the intrusions, and is concentrated along regional-scale, deep-seated structures such as the Cloncurry fault (e.g., De Jong and Williams, 1995; Mark and De Jong, 1996).

Lightning Creek: The Lightning Creek Cu-Au prospect is hosted by ca.1540 to 1500 Ma (Page and Sun, 1998) intrusive rocks, largely made up of sodic-calcic-altered quartz monzodiorite (Table 2; Perring et al., 2000). The addition of Na and Ca was caused by high temperature (>500°C) waters with a composition similar to primary magmatic fluid; K, Fe, and Cu were removed during the alteration process (Fig. 5; Tables 3 and 4; Perring et al., 2000). Quartzo-feldspathic and aplitic sills cut the altered intrusive rocks and were emplaced contemporaneously with the development of a large magnetite-rich ± Cu-Au vein system.

The sills are interpreted to be late-stage differentiates that crystallized under hydrous conditions with the episodic release of a fluid phase (Perring et al., 2000). The released fluid underwent phase separation that resulted in CO_2-rich vapor and a hypersaline (33–55 wt.% NaCl eq.) aqueous phase (Williams et al., 1999; Perring et al., 2000). The hypersaline fluid contained significant amounts of Fe (~10 wt.%) and Cu (~1 wt.%) plus Na, Ca, K, Cl, and Ba, and led to the formation of Ca-Fe ± Na alteration (pyroxene-albite ± magnetite) within the sills, and quartz-magnetite ± clinopyroxene ± albite ± pyrite ± chalcopyrite veins outside the sills (Williams et al., 1999; Perring et al., 2000). Calculated $\delta^{18}O_{water}$ values for quartz in the quartz-magnetite veins range from 7.8‰ to 9.9‰, and sulfur isotope values for pyrite and chalcopyrite in the veins range from –4.9‰ to –3.3‰ (Fig. 6; Williams et al., 1999; Perring et al., 2000). A later generation of calcite veins containing traces of Cu-Au mineralization probably crystallized from cooler (<200°C), more dilute (15–28 wt.% NaCl eq.) fluids that may include a meteoric component (Perring et al., 2000).

Eloise: The Eloise deposit is hosted within altered and deformed meta-arkose, quartz-biotite schist, and amphibolite of the Soldiers Cap Group (Table 2; Baker, 1996, 1998). No granitic rocks have been found in the Eloise area, but a large gravity low 10 km east of the deposit may be a pluton related to the Williams Batholith (Baker, 1998). The deposit occurs proximal to a bend in a regional shear zone (Baker, 1996) and metasomatism and mineralization are interpreted to have occurred synchronous with ductile-brittle deformation during the waning stages of the Isan Orogeny and emplacement of the Williams and Naraku batholiths (ca. 1540–1490 Ma; Baker and Laing, 1998). Mineralization is dominantly pyrrhotite-chalcopyrite and occurs in veins, silicified zones, and massive sulfide bodies within highly strained albite ± hornblende ± biotite-altered metasedimentary rocks proximal to and within the Eloise shear zone (Table 1; Baker, 1998; Baker et al., 2001). Gold is associated with chalcopyrite.

Fluids that formed the pervasive pre-mineralization albite and hornblende-biotite assemblages were high-temperature (400°–600°C), highly saline (≥26–68 wt.% total salts) brines (Fig. 5, Table 4; Baker, 1996; 1998). Copper-gold-bearing assemblages were precipitated from lower temperature (200°–450°C), lower salinity (30–47 wt.% total salts) fluids. Calculated oxygen isotope values for water in equilibrium with pre-mineralization assemblages and Cu-Au-bearing assemblages overlap those of typical magmatic and metamorphic fluids (Fig. 6; Baker et al., 2001). Sulfur isotope values for pyrite, chalcopyrite, and pyrrhotite range from 0.0‰ to 2.3‰, consistent with a

magmatic source for sulfur (Fig. 6).

The source of fluids is interpreted to be magmatic based on the high salinity of the fluids and the magmatic signature of the isotope data (Baker et al., 2001). Metals were likely carried as chloride complexes with H_2S as the dominant sulfur species, and ore deposition is interpreted to have been predominantly controlled by decreasing fluid temperature and the sulfidation of early Fe-rich alteration.

Hybrid Magmatic—Non-magmatic IOCG Systems

Hybrid magmatic–non-magmatic IOCG systems are generally spatially and/or temporally associated with igneous rocks, and fluid circulation is typically driven by the heat associated with magmatism. However, isotopic and geochemical data indicate input from non-magmatic (e.g., basinal brines), as well as magmatic fluids. The non-magmatic fluids are commonly highly saline and may be evaporite-derived (Barton and Johnson, 1996, 2000; Barton et al., 2000; Yardley and Graham, 2002). Either, or both, fluid types may be a source of metals and/or sulfur.

A large number of IOCG deposits fall into this category, and those chosen here represent the biggest known examples: Olympic Dam (Haynes et al., 1995), Candelaria (Ullrich and Clark, 1999), Salobo (Souza and Vieira, 2000), and Ernest Henry (Mark et al., 2000; Fig. 1; Table 1). One of Europe's most important copper producers, the enigmatic Aitik deposit, is also included in the list of examples. This deposit has characteristics of porphyry copper and IOCG deposits and may have formed from a combination of magmatic and evaporite-derived fluids as suggested by Wanhainen et al. (2003). Summary descriptions of the example deposits are presented below in order of deposit size.

Olympic Dam: The Olympic Dam deposit occurs in the eastern part of the Gawler Craton, a region largely underlain by ca. 1845 Ma deformed granite (Donnington suite), unconformably overlain by metasedimentary and metaigneous units of the Wallaroo Group (Fig. 1; Table 1; Creaser, 1995; Ferris et al., 2002). Dominantly felsic lavas and ignimbrites, and minor mafic lavas of the Gawler Range volcanics overlie the Wallaroo Group, and are intruded by and/or are coeval with (ca. 1595–1575 Ma) Hiltaba suite K feldspar-dominant granite to granodiorite (Ferris et al., 2002). The deposit formed at shallow depth during the late stages of intrusion of voluminous, felsic melts ca. 1590 Ma (Table 2; Roberts and Hudson, 1983; Oreskes and Einaudi, 1990; Reeve et al., 1990; Cross et al., 1993; Oreskes and Hitzman, 1993; Haynes et al., 1995; Johnson and Cross, 1995; Reynolds, 2000; Skirrow and Walshe, 2002; Williams and Pollard, 2003).

Olympic Dam is hosted by fractured, hematite-sericite-altered granite over an approximately 7 × 3 km area, and is associated with a zone of dilation related to a regional-scale fault zone (see references above). The deposit consists of multi-stage hematitic breccias around a core of barren hematite-quartz breccias. Mineralization was broadly contemporaneous with brecciation (Oreskes and Einaudi, 1990; Reeve et al., 1990) and occurs dominantly within breccia matrix as disseminated Cu-Fe sulfides and uraninite (Roberts and Hudson, 1983; Oreskes and Hitzman, 1993; Reynolds, 2000). Multiple mineralizing episodes have occurred, and each has the following general paragenetic assemblages (Oreskes and Einaudi, 1990; Haynes et al., 1995): (a) magnetite (± hematite), chlorite, sericite, siderite, and minor pyrite, chalcopyrite, and uraninite; (b) hematite, sericite, chalcocite, bornite, pitchblende, barite, fluorite, and chlorite; and (c) hematite, or hematite + quartz ± barite (Table 3). Assemblages (a) to (c) overlap in time and space, and there is a transition from chalcopyrite-bearing assemblages to bornite-(± chalcocite)-bearing assemblages about 100 to 300 m below the top of the deposit that locally follows upflow zones.

The repeated brecciation and alteration events that occurred during the formation of the Olympic Dam deposit created complex zoning and structural patterns that make it difficult for any one study area to be representative of the whole deposit. This has led to significant differences in detailed published accounts of the geology, and to a number of contrasting models for ore formation. Most models indicate formation from a combination of magmatic and non-magmatic fluids (e.g., Roberts and Hudson, 1983; Oreskes and Einaudi, 1990, 1992; Reeve et al., 1990; Haynes et al., 1995), but at least one model (Johnson and Cross, 1991) suggests that fluids were dominantly magmatic.

Interaction between hot, saline, relatively reduced, metal-bearing brine and cooler, oxidized saline meteoric waters was proposed by Reeve et al. (1990). Haynes et al. (1995) proposed a model involving the repeated mixing of hot, relatively oxidized, iron-rich, F-Ba-CO_2-bearing hydrothermal fluid (magmatic or deeply circulated meteoric water derived from a felsic volcanic or granitic source) with cooler, highly oxidized meteoric or connate fluid that contained Cu, U, Au, Ag, and sulfate derived from the interaction of saline lacustrine (or ground) water with mafic volcanic rocks. Oreskes and Einaudi (1990, 1992) suggested that the fluids that deposited early magnetite were hot (~400°C), had oxygen isotope characteristics ($\delta^{18}O_{water}$ = 8‰–10‰) similar to those of primary magmatic fluid or deeply circulating fluid that had equilibrated with metamorphic basement, were possibly highly saline (31–42 wt.% NaCl eq.), and carried Fe, Cu, and other metals (Figs. 5, 6; Table 4). They suggested that the hot fluids were followed by cooler (200°–400°C), lower salinity fluids with low $\delta^{18}O_{water}$ values (–2.5‰ to +4.5 ‰), which may have been derived from surficial fluids (evolved meteoric, closed-basin, groundwater, and/or seawater). Johnson and Cross (1991) presented a model based on Sm-Nd isotopic evidence that involved two fluids: (1) fluid in isotopic equilibrium with Hiltaba suite granites, which led to the precipitation of early magnetite; and (2) fluid derived from an ascending volatile phase exsolved from mafic/ultramafic magma and enriched in Cu and REE, which led to the precipitation of Cu mineralization. Reynolds (2000) suggested that both ore fluids and metals had magmatic sources, and Knutson et al. (1992) reported that Mesoproterozoic basalts were a possible source of Cu.

Sulfur isotope data indicate average $\delta^{34}S$ values of pyrite

= –6‰, chalcopyrite = –7‰, bornite = –7‰, chalcocite = –10‰, and barite = +11‰ (Eldridge, 1994). Differences between sulfur isotope values for different minerals are broadly compatible with a temperature of formation of approximately 300°C. Bimodal results for sulfur isotope data in an area with elevated gold values suggest boiling may have been important in gold deposition (Eldridge, 1994).

Aitik: The Aitik deposit is located in northern Fennoscandia in a 40 × 5 km NNW-trending belt of Cu-(Au) mineralization (Fig. 1; Table 1; Frietsch et al., 1997; Carlon, 2000). The mineralized belt is spatially associated with a regional-scale fault/shear zone and is underlain by ca. 1910 to 1880 Ma metavolcanic rocks (Table 2; Skiöld and Cliff, 1984; Skiöld, 1987; Frietsch et al., 1997; Carlon, 2000). Copper-(Au) mineralizing events within the belt are interpreted to be related to large-scale Na-Cl-rich fluid fluxes synchronous with granitic igneous activity at ca. 1890 to 1860 Ma and ca. 1830 to 1770 Ma (sources as above).

Aitik is hosted by metamorphosed intermediate composition volcanic rocks and clastic sedimentary rocks that have been affected by pervasive sericite, scapolite, and tourmaline alteration (Table 3; Frietsch et al., 1997; Wanhainen et al., 2003). The deposit exhibits multiple phases of brittle-ductile deformation and its location is controlled by a NNW-trending fault zone (Frietsch et al., 1997; Carlon, 2000; Wanhainen et al., 2003). Chalcopyrite and pyrite with minor magnetite, pyrrhotite, bornite, chalcocite, and molybdenite occur as disseminations and stringers in garnet-bearing biotite schist and gneiss and muscovite schist (Frietsch et al., 1997; Wanhainen and Martinsson, 1999; Carlon, 2000; Wanhainen et al., 2003). Stockwork quartz-chalcopyrite-pyrite veins extend into ca. 1870 Ma quartz monzodiorite that occurs in the footwall. Native gold and gold alloys occur with chalcopyrite and pyrite and are intergrown with non-sulfide minerals (Wanhainen et al., 2003).

Chalcopyrite mineralization was deposited prior to bornite from moderate temperature (140°–373°C), highly saline (31–37 wt.% NaCl eq.) fluids (Fig. 5; Table 4; Wanhainen et al., 2003). Bornite mineralization was deposited from moderate-temperature (100°–222°C), less saline (18–27 wt.% NaCl + $CaCl_2$ eq.) fluids. Sulfur isotope values for pyrite and chalcopyrite range from –3.4‰ to +3.3‰, and from +6.7‰ to +13.8‰ for barite (Fig. 6; Frietsch et al., 1995).

The Aitik deposit has been interpreted to be genetically related to hydrothermal fluids exsolved from the underlying syntectonic quartz monzodiorite (Monro, 1988), with a contribution to the fluid from evaporitic sources (Wanhainen et al., 2003). Based on isotopic data, sulfur is interpreted to have been derived either from magmatic fluid or the dissolution of igneous sulfides (Fig. 6; Frietsch et al., 1995). The high calcium and sodium content of fluid inclusions related to the main chalcopyrite mineralizing event is interpreted to indicate that at least some fluid was derived from evaporitic sources (Wanhainen et al., 2003). Highly saline hydrothermal fluids derived from an evaporitic source have also been invoked to explain pervasive scapolite and albite alteration that is widespread in the region (Frietsch et al., 1997).

Candelaria: The Candelaria Cu-Au deposit is located within an approximately 5 × 20 km belt of IOCG and iron deposits that occurs in an area underlain by an Early Cretaceous continental arc and marine back-arc basin terrane (Fig. 1; Table 1; Ullrich and Clark, 1999; Marschik et al., 2000; Marschik and Fontboté, 2001). The deposit is hosted by andesitic volcanic flows and volcaniclastic breccias overlain by limestones and minor evaporites, and is proximal to the composite Copiapó Batholith (Table 2; Ullrich and Clark, 1999). Formation of the deposit was broadly contemporaneous with mid-Cretaceous uplift and batholith emplacement (Ullrich and Clark, 1999; Mathur et al., 2002).

Mineralization occurs largely as veins and breccia infill, and is concentrated at the intersection of brittle faults with a contact between relatively impermeable and overlying permeable volcanic rocks (Marschik and Fontboté, 1996, 2001; Ullrich and Clark, 1999; Marschik et al., 2000). Intense, high temperature (500°–600°C), biotite-quartz-magnetite alteration preceded the main Cu-Au mineralizing event (Table 4), which was associated with Ca-Na metasomatism. Ore consists mainly of magnetite and/or hematite, chalcopyrite, and pyrite, locally abundant pyrrhotite and sphalerite, and trace amounts of molybdenite and arsenopyrite. Gold occurs as inclusions in chalcopyrite, in fractures within pyrite, and as Hg-Au-Ag alloy. Gangue consists mainly of quartz and anhydrite.

Main-stage Cu-Au mineralization is associated with quartz containing hypersaline and CO_2-rich fluid inclusions with homogenization temperatures from ~330° to 440°C (Fig. 5, Table 4; Ullrich and Clark, 1999; Marschik et al., 2000). Sulfur isotope values for main ore-stage sulfides range from –1.3‰ to +5.7‰, and from 14.5‰ to 17.5‰ for anhydrite associated with the chalcopyrite (Fig. 6; Ullrich and Clark, 1999; Marschik and Fontboté, 2001). Oxygen isotope values for fluid in equilibrium with ore-stage quartz at Candelaria range from approximately 6‰ to 9‰ (Fig. 6; Marschik and Fontboté, 2001). Late-stage calcite contains fluid inclusions with homogenization temperatures of ≤236°C. $\delta^{34}S$ values for late-stage chalcopyrite range from 0.8‰ to 7.2‰, and $\delta^{18}O_{fluid}$ values in equilibrium with late-stage calcite range from –5.4‰ to +1.3‰ (Ullrich and Clark, 1999; Marschik and Fontboté, 2001).

A magmatic fluid contribution to the hydrothermal system that formed the Candelaria deposit is indicated by the calculated fluid oxygen isotope values, the presence of both hypersaline and CO_2-rich fluid inclusions, the oxidized nature of the ore fluid as indicated by early formed hematite, coeval ages for mineralization and intrusive activity, similar Pb isotope values for sulfides and volcanic and intrusive rocks, and similar initial $^{187}Os/^{188}Os$ ratios for magnetite, sulfides, and magmatic magnetite (Marschik et al., 2000; Marschik and Fontboté, 2001; Mathur et al., 2002). The presence of non-magmatic fluid (basinal brines, formation or meteoric waters) is inferred from the low calculated $\delta^{18}O$ values for fluid in equilibrium with calcite, and from sulfur isotopic data, which indicate that early, reduced, Cu-de-

positing fluids with near magmatic S compositions ($\delta^{34}S_{fluid}$ = –1.3‰ to +5.7‰ early in the main Cu-Au event) were replaced by more oxidized and probably evaporite-sourced brines ($\delta^{34}S_{fluid}$ = 11.7‰ to 16.8‰ late in the main Cu-Au event; $\delta^{34}S_{fluid}$ = 13‰ to 20.2‰ in late-stage calcite-anhydrite; Ullrich and Clark, 1999). These observations suggest that the main ore-forming event may have been dominated by the mixing of sulfur-bearing fluids from magmatic and evaporitic sources (Ullrich and Clark, 1999).

Salobo: The Carajás metallogenic province in Brazil is host to Salobo (Fig. 1, Table 1) and a number of other Fe oxide Cu-Au (± Mo, Ag, U, REE) deposits including Igarapé Bahia, Alemão, Cristalino, Sossego, Águas Claras, and Gameleira (Tazava and de Olivera, 2000; Marschik et al., 2005). The deposits occur within the Carajás basin, which is underlain by Neoarchean (ca. 2750 Ma) volcano-sedimentary rocks of the Itacaiúnas Supergroup, unconformably overlain by ca. 2680 Ma marine siliciclastic rocks of the Águas Claras Formation or Rio Fresco Group, all of which were likely deposited in an extensional environment (DOCEGEO, 1988; Lindenmayer, 1990; Machado et al., 1991; Pinheiro, 1997; Villas and Santos, 2001). Rocks within the basin were intruded by ca. 2750 Ma mafic-ultramafic (Luanga complex) and granitoid (Estrela complex) rocks, ca. 2740 Ma granitoids and diorites (Plaquê suite), ca. 2570 Ma granite (Old Salobo granite), and ca. 1880 Ma granitoids (Carajás suite; Machado et al., 1991; Barros et al., 1997). The IOCG deposits are associated with abundant magnetite and/or hematite, are structurally controlled, and are enriched in LREE, Co, Ni, Pb, Zn, As, Bi, W, and U (Requia and Fontboté, 2000; Ronzê et al., 2000; Souza and Vieira, 2000; Tazava and de Olivera, 2000).

The Salobo deposit is situated at the western termination of the Cinzento transcurrent system and is located within a lens of Itacaiúnas Supergroup bounded by basement gneiss (Table 2; Pinheiro, 1997; Souza and Vieira, 2000). The deposit is hosted by metagreywackes that contain lenses or layers of amphibolite (Requia and Fontboté, 2000) and are cut by ca. 2570 (Old Salobo Granite) and ca. 1880 Ma (Young Salobo Granite) granitoids, and ca. 550 to 560 Ma diabase dikes (Machado et al., 1991; Souza and Vieira, 2000). Crosscutting relationships demonstrate that mineralization at Salobo is post-metamorphic. Isotopic dating, based on Re-Os and Pb-Pb analyses of sulfides and magnetite, indicates an age of ca. 2570 Ma for the mineralization, roughly coeval with emplacement of Old Salobo granite (e.g., Machado et al., 1991; Souza and Vieira, 2000; Requia et al., 2003).

Mineralization occurs along a NW-trending shear zone and consists dominantly of steeply-dipping lenses of: (1) abundant early magnetite with minor hematite and local graphite; and (2) less abundant, later chalcopyrite, bornite, and chalcocite (Machado et al., 1991; Requia and Fontboté, 2000; Souza and Vieira, 2000; Requia et al., 2003). Copper sulfides also occur in veins cutting iron-rich rocks. Accessory minerals include hematite, molybdenite, ilmenite, uraninite, digenite, and covellite; native gold occurs as inclusions in cobaltite, safflorite, and copper sulfides, or interstitial to magnetite and chalcopyrite grains (Machado et al., 1991; Souza and Vieira, 2000).

Alteration around the deposit includes early Na-metasomatism (Na-plagioclase) overprinted by extensive K-metasomatism (K feldspar, biotite; Requia and Fontboté, 2000; Requia et al., 2003). Intense K-Fe-metasomatism is spatially associated with the main ore zone (Requia et al., 2003). Propylitic alteration overprints earlier phases and is characterized by the infiltration of Ca-bearing fluids. Veinlets with quartz, stilpnomelane, fluorite, allanite, chalcopyrite, molybdenite, cobaltite, and gold formed during propylitic alteration (Lindenmayer, 1990; Souza and Vieira, 2000). Chloritization associated with brittle shearing accompanied the propylitic alteration (Lindenmayer, 1990; Souza and Vieira, 2000).

The interaction of a mixture of magmatic and connate brines with a more oxidized fluid is suggested as an ore-forming mechanism, and sulfur isotope values of 0.2‰ to 1.6‰ suggest a predominantly magmatic source for sulfur (Fig. 6; Requia and Fontboté, 2000).

Ernest Henry: The Ernest Henry deposit (Table 1), like the magmatic end-member Lightning Creek and Eloise deposits, occurs in the Cloncurry district of Australia (Fig. 1). The deposit is hosted predominantly by ca. 1740 Ma plagioclase-phyric meta-andesitic volcanic rocks that are locally intercalated with siliciclastic, calc-silicate-rich (scapolite-bearing), and graphitic metasedimentary rocks; ca. 1660 Ma metadiorite also occurs in this area (Table 2; Mark et al., 2000, 2006). Host rocks have been affected by: (1) Na-Ca alteration characterized by hematite-bearing albite; and (2) disseminated biotite-magnetite alteration and garnet-K feldspar-biotite alteration (Ryan, 1998; Mark et al., 2000, 2006). Mineralization was roughly coeval with emplacement of the Williams and Naraku batholiths at ca. 1540 to 1500 Ma (Blake et al., 1990; Ryan, 1998; Mark et al., 2000, 2006; Williams et al., 2005), and is associated with extensive K feldspar-hematite alteration (Table 3; Ryan, 1998; Mark et al., 2000, 2006). Post-ore alteration is dominated by carbonate.

The location of the orebody is structurally controlled, and occurs within volcanic rocks that were brecciated during reverse fault movement along bounding shear zones (Mark et al., 2000). Breccia infill is made up dominantly of a magnetite-carbonate-sulfide assemblage, but also contains biotite, K feldspar, hematite, garnet, barite, fluorite, and quartz (Ryan, 1998; Mark et al., 2000). Primary and supergene mineralized zones are present. Chalcopyrite and pyrite are the dominant sulfide minerals in the primary zone. Chalcocite, hematite, calcite, and siderite are abundant in the supergene zone. There is a strong correlation between copper and gold in the primary zone, but gold is largely decoupled from copper in the weathered zone. Anomalous amounts of cobalt, molybdenum, uranium, REE, arsenic, fluorine, and barium are associated with the copper mineralization in both zones (Ryan, 1998; Mark et al., 2000).

Ore fluids were high temperature (~350°–450°C) and high salinity (>26 wt.% NaCl eq.; Fig. 5; Table 4; Mark et al., 2000, 2006). Stable isotope data are compatible with a

significant magmatic contribution to ore-forming fluid(s) and/or sulfur ($\delta^{34}S_{chalcopyrite}$ = –1‰ to +4‰; $\delta^{18}O_{fluid}$ = 8‰ to 11‰; Fig. 6; Mark et al., 2000, 2006). However, the wide range of elements enriched in Ernest Henry ore (Table 1) suggests involvement of more than one fluid. Copper and Au (+ Fe, Ba) were probably carried as chloride complexes, and pyrite and chalcopyrite (plus magnetite and barite) were likely deposited via a mechanism(s) that involved fluid mixing, changes in pressure, and/or cooling during brecciation (Mark et al., 2000, 2006).

Discussion

Iron oxide copper-gold deposits do not appear to form in any one specific geological setting (Tables 1–4, and references therein). They are found in a variety of environments that are able to provide basic ingredients for formation: hot, saline (dominantly oxidized) fluid(s), permeable flow paths (e.g., faults, shear zones, permeable lithologies), source(s) of metals and sulfur (either in original fluid or leached from rocks en route), mechanism(s) to drive fluid flow (e.g., heat, tectonics, gravity, density gradients), traps for metal precipitation (e.g., breccia zones), and means to precipitate ore minerals (e.g., fluid mixing, cooling, changes in pH and/or f_{O_2}). Thus, unlike other types of mineral deposits which form in a restricted range of geological environments (e.g., volcanic-associated massive sulfide, skarn, Mississippi Valley-type), IOCG deposits can form in a variety of environments ranging from those containing abundant igneous rocks (e.g., Lightning Creek, Olympic Dam) to those with large volumes of igneous and sedimentary rocks (e.g., Cloncurry), to those dominated by sedimentary rocks (e.g., Wernecke Breccia). The type of alteration and mineralization in any IOCG district or at any one deposit will be affected by, for instance, the abundance of fluid of various types (e.g., magmatic, metamorphic, basinal, meteoric), the composition of host strata (e.g., igneous rocks, evaporites), the degree of interaction between fluid and rocks along the fluid pathway (e.g., function of fluid temperature, pH, f_{O_2}), and the degree of permeability of the host rocks (e.g., presence of major structures to act as fluid paths, or permeable lithologies; Williams and Blake, 1993; Barton and Johnson, 1996, 2000). Thus, IOCG systems can be viewed as forming a spectrum of deposits ranging from those dominated by magmatic environments and fluids, to those where non-magmatic fluids dominate in an amagmatic environment, as illustrated in Figure 7.

Comparison of IOCG systems

Tectonic Setting: In general, IOCG deposits occur in extensional settings (e.g., Hitzman et al., 1992). For example, Candelaria, Aitik, and possibly Olympic Dam were emplaced within arc–back-arc systems above subducting slabs (Gorbatshev and Bogdanova, 1993; Ullrich and Clark, 1999; Marschik et al., 2000; Marschik and Fontboté, 2001; Ferris et al., 2002), and deposits within the Carajás and Wernecke regions likely formed in continental rift environments (DOCEGEO, 1988; Lindenmayer, 1990; Machado et al., 1991; Pinheiro, 1997; Thorkelson, 2000; Thorkelson et al., 2001b). The deposits are largely coeval with tectonic activity, are spatially related to regional-scale fault and/or shear zones, and also exhibit structural control on a smaller scale (Table 2, and references therein). For example, the Ernest Henry and Olympic Dam deposits occur in dilational zones, the ore zone at Candelaria is located at the intersection of shear/fault zones with a lithological contact between relatively impermeable rocks and overlying permeable strata, and Wernecke Breccia mineralization occurs in structurally weak, permeable zones such as fractured fold hinges (references given above).

Host Rocks: IOCG systems are not restricted to particular types of host rocks and can occur in intrusive, volcanic, sedimentary, and ironstone hosts (Table 2, and references therein). As noted above, magmatic and hybrid IOCG systems are temporally and, generally, spatially related to intrusive rocks. Non-magmatic IOCG systems are not temporally related to igneous rocks, but may be spatially related, for example, Wernecke Breccia. A single area may host various types of IOCG systems. For example the Cloncurry district is host to magmatic (Lightning Creek, Eloise) and hybrid (Ernest Henry) systems (Tables 1–4, and references therein), indicating that different fluid pathways and sources were present in the area. The extension of this district, the Tennant Creek inlier, hosts non-magmatic IOCG systems (e.g., Skirrow and Walshe, 2002). The presence of evaporites in the host rock package appears to be important (Haynes et al., 1995; Barton and Johnson, 1996, 2000; Hitzman, 2000). For example, Wernecke Breccia is most abundant proximal to a metahalite horizon (Hunt, 2005) and new Br/Cl data for the Eloise and Osborne (Cloncurry district) deposits suggests a variable but significant contribution of evaporitic halite to the fluid (Williams et al., unpub. data, 2006).

Alteration: Most IOCG systems are associated with regional, pervasive alteration (Table 3, and references therein). For example, as noted above, extensive sodic-calcic alteration occurs in the Cloncurry district, widespread sodic alteration occurs in the Aitik and Candelaria regions, and Salobo, Wernecke Breccia, and Redbank are associated with abundant sodic and/or potassic alteration. Extensive hematite-sericite-chlorite alteration occurs in the Olympic Dam area (Reynolds, 2000). In general, late alteration in IOCG systems is dominated by carbonate (Table 3, and references therein).

Fluid Composition, Temperature, and Salinity: IOCG deposits were formed by moderate- to high-temperature, complex brines, largely made up of H_2O, NaCl, and $CaCl_2$ (Table 4, and references therein). The fluids were varied, and different brine compositions may occur within a deposit, between deposits in a given district, and between districts. The sulfur content of the brines was typically low and oxygen fugacity was variable.

In general, early-stage alteration in magmatic IOCG systems formed from high-temperature, high-salinity fluids

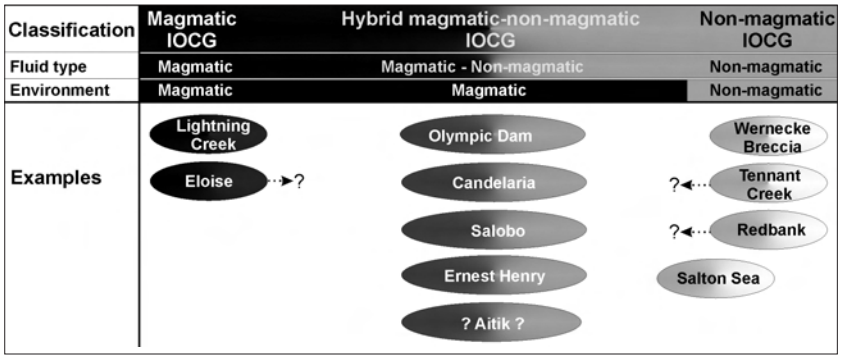

Fig. 7. Suggested classification of IOCG systems into magmatic and non-magmatic end members, with hybrid IOCG systems in between. Also shown are examples for each IOCG category. See text for discussion and references.

(Fig. 5). For example, pre-ore albite and hornblende-biotite alteration at Eloise formed from 400° to 600°C fluids with a salinity of ≥26 to 68 wt.% total salts (Tables 1–4, Figs. 5–6, and references therein). Early phases in some hybrid magmatic–non-magmatic IOCG systems also formed from fluids with high temperatures and salinities, for example, pre-Cu-Au (main stage) biotite-quartz-magnetite alteration at Candelaria, and early magnetite at Olympic Dam (Tables 1–4, Figs. 5, 6, and references therein). Fluid temperature and salinity generally decreased towards later stages, and differences between IOCG types are less apparent. For example, mineralization-stage fluid temperature varied from approximately 200° to greater than 500°C, 100° to 450°C, and 185° to 350°C, and salinity ranged from 33 to 55 wt.% NaCl eq., 18 to 37 wt.% NaCl eq., and 3 to 42 wt.% NaCl eq., respectively, for magmatic, hybrid magmatic–non-magmatic, and non-magmatic IOCG systems listed in Tables 1 and 4.

Oxygen Isotopic Composition of Fluid: Calculated $\delta^{18}O_{fluid}$ values for magmatic IOCG systems generally overlap values for magmatic fluid (5‰–10‰; Fig. 6, and references therein). For example, $\delta^{18}O_{fluid} \approx$ 8‰ to 10‰, and 5‰ to 10‰, respectively, for Lightning Creek and Eloise. Fluids related to hybrid magmatic–non-magmatic IOCG systems show a wider range of isotopic compositions that commonly vary temporally from early magmatic values, to those reflecting the later input of other fluids (Fig. 6). For example, $\delta^{18}O_{fluid} \approx$ 8‰ to 10‰, and –2‰ to +5‰ for fluid in equilibrium with early magnetite and later hematite, respectively, at Olympic Dam (Oreskes and Hitzman, 1993). At Candelaria, $\delta^{18}O_{fluid} \approx$ 6‰ to 9‰ for ore stage mineralization, and $\delta^{18}O_{fluid} \approx$ –5‰ to +2‰ for later mineralization (Marschik and Fontboté, 2001). Non-magmatic IOCG systems have a wide range of fluid oxygen isotopic compositions: for example, $\delta^{18}O_{fluid} \approx$ 0‰ to +16‰ and –7‰ to +14‰ respectively for Redbank and Wernecke Breccia (Knutson et al., 1979; Hunt, 2005).

Sulfur Isotopes: Sulfur isotope values for magmatic IOCG systems are generally close to those of mantle-derived sulfur (Fig. 6): for example, $\delta^{34}S$ = 0‰ to 2.3‰ at the Eloise deposit (Baker, 1998). Some hybrid magmatic–non-magmatic IOCG systems also have sulfur isotopic compositions close to those of mantle-derived sulfur, but others show a wider range. Non-magmatic IOCG systems have a wide range of sulfur isotope values: for example, $\delta^{34}S$ values for chalcopyrite and pyrite from Wernecke Breccia range from –12‰ to +14‰ (Hunt, 2005), and $\delta^{34}S$ values for the main copper mineralization at Redbank vary from +4‰ to +16‰. In general, the large hybrid IOCG systems shown in Figure 6 do not show as large a variation in sulfur isotopic compositions as the non-magmatic IOCG systems, although Eldridge (1994) reports one $\delta^{34}S$ value of –47‰ from Olympic Dam. However, at least one small hybrid IOCG system has a wide range of sulfur isotope compositions: pyrite and chalcopyrite from Monakoff, which is interpreted to have formed from the mixing of granite-derived and metaevaporite-derived fluids, returned $\delta^{34}S$ values of –10‰ to +12‰ (Davidson et al., 2002).

Deposit Size and Grade: Mineralization occurs dominantly as disseminations, veins, and breccia infill in all IOCG types. However, the size of deposits varies widely (Table 1, and references therein). In general, based on the examples listed in Table 1, magmatic IOCG deposits tend to be small and higher grade. For example, Eloise has a resource of 3.2 Mt of 5.8 wt.% Cu, 1.5 g/t Au, and 19 g/t Ag (Baker and Laing, 1998). Hybrid deposits are generally low grade, but have the potential to be very large: for example, Olympic Dam is reported to have had a pre-mining resource of 2320 Mt of 1.3 wt.% Cu, 0.5 g/t Au, 2.9 g/t Ag, and 0.4 kg/t U_3O_8 (Reeve et al., 1990). Non-magmatic IOCG deposits can be small to medium in size, and high or low grade (Table 1). Most IOCG systems contain a variety of associated elements including cobalt, molybdenum, REE, and bismuth (Table 1, and references therein). Eloise and Olympic Dam are reported to contain Ni, which may reflect a primitive magmatic contribution (Reynolds, 2000; Baker et al., 2001).

Mechanisms that would cause the precipitation of ore minerals include: fluid mixing, possibly with less saline, oxidized, and/or sulfur-bearing fluid (Table 4; e.g., Barton and Johnson, 1996, 2000; Williams et al., unpub. data, 2006); CO_2-brine unmixing (e.g., Osborne deposit; Adshead, 1995; Mustard et al., 2003); and the sulfidation of pre-existing iron silicates (e.g., Eloise; Baker, 1998). Recent work by Liu and McPhail (2005) has demonstrated the importance of decreasing temperature in the precipitation of chalcopyrite from hydrothermal fluids at the Starra IOCG deposit. The presence of abundant fluid (i.e., magmatic + other sources) and a magmatic source of heat ± metals ± sulfur (e.g., Barton and Johnson, 2000) may account for the large tonnage potential of hybrid systems. During fluid circulation, Fe and base metals could be leached from host rocks along the fluid pathway. For example, in the Clon-

curry district, K, Fe, and Cu were leached from host rocks during widespread sodic-calcic alteration creating a fluid with the potential to contribute to the overall metal budget of the district (Williams and Blake, 1993; De Jong and Williams, 1995; Adshead et al., 1998; Baker, 1998; Rotherham et al., 1998; Mark et al., 2000; Perring et al., 2000). Metals and/or sulfur could also be supplied by magmatic fluid: for example, PIXE analyses of fluid inclusions from the Lightning Creek deposit indicate a copper content of up to 1 wt.% (Perring et al., 2000; Williams et al., unpub. data, 2006). In magmatic environments, fluid flow tends to be focussed into permeable zones, and fluid generally cools rapidly as it migrates away from the heat source (Barton and Johnson, 2000). The rapid cooling causes precipitation of sulfides, and the focused flow concentrates precipitation in a relatively limited area. The amount of sulfides precipitated would be limited largely by the sulfur content of the fluid. In end member magmatic IOCG systems, fluid is derived from plutons and may be less abundant, leading to smaller, more focused deposits. In non-magmatic environments, fluid flow may not be as focused, and widely disseminated sulfides may result, rather than concentrated sulfide deposits. Metal grades may also be lower because there is no highly concentrated contribution from magmatic fluid. In all cases, metals present in the fluid will be lost if the sulfur content is low and/or if there is no favorable trap.

Relationship to Other Deposit Types

Non-magmatic end-member IOCG systems have potential links to other sediment-hosted copper systems, such as the Mount Isa Cu deposit and deposits in the Zambian copper belt. The Wernecke Breccia and Mount Isa Cu deposits occur in rift-related settings (O'Dea et al., 1997; Betts et al., 1998; Thorkelson, 2000). They are hosted by thick sedimentary packages that contained evaporite horizons and carbonaceous, pyritic shale. Breccia-hosted mineralization is structurally controlled and at least partly synchronous with tectonic activity (Delaney, 1981; Perkins, 1984, 1990; Swager, 1985; Heinrich et al., 1989, 1995, 2000; Perkins et al., 1999; Thorkelson et al., 2001b; Davis, 2004; Matthai et al., 2004; Hunt, 2005). Deposits within the Zambian copper belt are also hosted by thick, evaporite-bearing sedimentary sequences, and are not temporally associated with igneous intrusions (e.g., Fleischer et al., 1976; Sweeney et al., 1986; Unrug, 1988; Annels, 1989). The mineralization is at least partly structurally controlled and recent work indicates some is synchronous with deformation (McGowan et al., 2003, 2006).

In each region, the onset of deformation may have been a driving force for the movement of hydrothermal fluids. All were formed from hot, high-salinity brines that indicate the involvement of evaporites, and were likely evolved basinal/metamorphic waters (e.g., Sverjensky, 1987; Heinrich et al., 1993, 1995; Hunt, 2005). Sulfur isotopic compositions for sulfides have a wide range of values in each area: –12‰ to +14‰; –7‰ to +24‰, and –17‰ to +23 ‰, respectively, for Wernecke Breccia, Mount Isa Cu, and the Zambian Copperbelt, indicating a dominantly non-magmatic source for sulfur (e.g., Andrew et al., 1989; McGowan et al., 2003; Hunt, 2005). Host-strata and/or proximal mafic rocks are likely sources of copper in each area (e.g., Annels, 1989; Heinrich et al., 1995; Hunt, 2005).

Non-magmatic IOCG systems are also somewhat similar (cf. Barton et al., 2000) to hematite-rich detachment fault-related mineralization in the southern Basin and Range Province, USA, as described by Wilkins et al. (1986). The syntectonic, amagmatic, detachment fault-related deposits occur in permeable (dilatant/brecciated) regions at varying distances from the fault zone. They contain oxide and sulfide facies and were largely formed from hot (200°–325°C), saline (12–20 wt.% NaCl eq.) basinal brines, with deposit components leached out of basin lithologies. Latent heat was provided to the system by lower plate rocks that were rapidly uplifted during Cenozoic extension. Syntectonic igneous intrusions are not considered by Wilkins et al. (1986) to be a feasible source of heat, because they are not abundant, and where they do occur they are significantly older than the mineralization.

The Salton Sea geothermal system, where iron oxide Cu-Au-REE (± Pb ± Zn) mineralization is precipitated from evaporite-derived hypersaline brines may be a modern analogue of a non-magmatic system (e.g., McKibben and Elders, 1985; McKibben and Hardie, 1997). However, this system occurs in a rifting environment, and fluid is interpreted to be circulated by igneous-driven convection. Thus, it cannot be considered an end-member non-magmatic IOCG system, but would lie between hybrid and end-member non-magmatic IOCG systems as shown on Figure 7.

End-member magmatic IOCG deposits are similar to some porphyry Cu-(Au) deposits (e.g., Pollard, 2000; Sillitoe, 2003; Williams et al., 2005). For example, Lightning Creek is associated with K-rich, magnetite-series, metaluminous intrusive rocks that are similar to intrusive rocks associated with Cu-Au porphyry systems (Pollard et al., 1998; Perring et al., 2000). Pollard (2000) suggested that the development of the two styles of mineralization was related to the composition of the granitoids and the evolution of the hydrothermal fluids; specifically, that boiling of magmatic-derived H_2O-salt fluids can lead to porphyry deposits, and unmixing of magmatic-derived H_2O-CO_2-salt fluids can lead to IOCG deposits. He suggests the variable CO_2 content of the magmas is a key factor in the evolution of the mineralizing system (see also Lowenstern, 2001).

Conclusions

New data for Wernecke Breccia-associated IOCG deposits indicate that the spectrum of magmatic and hybrid magmatic–non-magmatic genetic modes typically invoked for the formation of IOCG deposits should be expanded to accommodate IOCG systems that formed in amagmatic environments. This has implications for IOCG exploration, in that the search can be expanded beyond the traditionally explored magmatic environments to include all areas underlain by evaporate-bearing sedimentary strata in

regions capable of producing elevated fluid temperatures (i.e., regions with above average geothermal gradients and/or sufficiently thick strata). Like magmatic environments, in addition to hot, saline (oxidized) fluid(s), prospective amagmatic areas also need to provide the other basic ingredients for deposit formation: permeable flow paths (e.g., faults, shear zones), source(s) of metals and sulfur (either in original fluid or leached from rocks en route), mechanism(s) to drive fluid flow (e.g., heat, tectonism, gravity, density gradients), traps for metal precipitation (e.g., breccia zones), and the means to precipitate ore minerals (e.g., fluid mixing, cooling, changes in pH and/or f_{O_2}).

A division of the broad class of IOCG deposits into end-member magmatic and non-magmatic IOCG systems, with hybrid magmatic–non-magmatic IOCG systems in between, would allow their attributes to be more narrowly defined and these could be used in exploration models. For example, large low-grade deposits such as Olympic Dam and Ernest Henry are hybrid IOCG systems. Magmatic end members are generally smaller, but can be higher grade (e.g., Eloise). Non-magmatic end members are small to medium in size and low to high grade.

End-member magmatic IOCG deposits, such as Lightning Creek, have similarities to some porphyry deposits (e.g., Pollard, 2000), whereas non-magmatic IOCG end members share characteristics with some sediment-hosted Cu-(Co-U) deposits (e.g., Mount Isa copper, Zambian Copperbelt), suggesting that the range of IOCG deposits may form a link between intrusive- and sediment-related deposits.

Acknowledgments

Support for this project was provided by the Yukon Geological Survey, an Australian International Postgraduate Research Scholarship, a James Cook University scholarship and Merit Research Grant, a Society of Economic Geologists Student Research Grant, and a Predictive Minerals Discovery Cooperative Research Centre (pmd*CRC) scholarship. Newmont Mining Corporation, Archer, Cathro & Associates (1981) Ltd., Equity Engineering, Pamicon Developments, Monster Copper Resources, and Blackstone Resources kindly provided access to confidential data, drill core, and/or properties. This paper benefited from constructive comments and suggestions by M. Jébrak, R. Tosdal, and D. Lentz.

References

Adshead, N.D., 1995, Geology, alteration, and geochemistry of the Osborne Cu-Au deposit, Cloncurry district, NW Queensland, Australia: Ph.D. Thesis, Townsville, Australia, James Cook University, 382 p.

Adshead, N.D., Voulgaris, P., and Muscio, V.N., 1998, Osborne copper-gold deposit, *in* Berkman, D.A., and Mackenzie, D.H., eds., Geology of Australian and Papua New Guinean mineral deposits: Melbourne, The Australasian Institute of Mining and Metallurgy, p. 793–799.

Ahmad, M., Wygralak, A.S., and Ferenczi, P.A., 1999, Gold deposits of the Northern Territory: Northern Territory Geological Survey Report, v. 11, 95 p.

Andrew, A.S., Heinrich, C.A., Wilkins, R.W.T., and Patterson, D.J., 1989, Sulfur isotope systematics of copper ore formation at Mount Isa, Queensland: Economic Geology, v. 84, p. 1614–1626.

Annels, A.E., 1989, Ore genesis in the Zambian copper belt, with particular reference to the northern sector of the Chambishi Basin, *in* Boyle, R.W., et al., eds., Sediment-hosted stratiform copper deposits: Geological Association of Canada, Special Paper 36, p. 427–452.

Baker, T., 1996, The geology and genesis of the Eloise Cu-Au deposit, Cloncurry district, NW Queensland, Australia: Ph.D. Thesis, Townsville, Australia, James Cook University, 200 p.

Baker, T., 1998, Alteration, mineralization, and fluid evolution at the Eloise Cu-Au deposit, Cloncurry district, northwest Queensland, Australia: Economic Geology, v. 93, p. 1213–1236.

Baker, T., and Laing, W.P., 1998, Eloise Cu-Au deposit, East Mount Isa block: Structural environment and structural controls on ore: Australian Journal of Earth Sciences, v. 45, p. 429–444.

Baker, T., Perkins, C., Blake, K.L., and Williams, P.J., 2001, Radiogenic and stable isotope constraints on the genesis of the Eloise Cu-Au deposit, Cloncurry district, northwest Queensland: Economic Geology, v. 96, p. 723–742.

Barros, C.E. de M., Dall'Agnoll, R., Barbey, P., and Boullier, A.M., 1997, Geochemistry of the Estrela granite complex, Carajás region, Brazil: An example of an Archaean A-type granitoid: Journal of South American Earth Sciences, v. 10, p. 321–330.

Barton, M.D., and Johnson, D.A., 1996, Evaporitic-source model for igneous-related Fe oxide-(REE-Cu-Au-U) mineralization: Geology, v. 24, p. 259–262.

Barton, M.D., and Johnson, D.A., 2000, Alternative brine sources for Fe-Oxide(-Cu-Au) systems: Implications for hydrothermal alteration and metals, *in* Porter, T.M., ed., Hydrothermal iron oxide copper-gold and related deposits: A global perspective, Volume 1: Adelaide, PGC Publishing, p. 43–60.

Barton, M.D., Johnson, D.A., and Zurcher, L., 2000, Phanerozoic iron oxide (REE-Cu-Au-U) systems in southwestern North America and their origins, *in* Roberts, M.D., and Fairclough, M.C., eds., Fe-oxide-Cu-Au deposits: A discussion of critical issues and current developments [abs.]: EGRU Contribution 58, Australia, James Cook University, Extended Symposium Abstracts, p. 5–11.

Beardsmore, T.J., Newbery, S.P., and Laing, W.P., 1988, The Maronan Supergroup: An inferred early volcano sedimentary rift sequence in the Mount Isa inlier, and its implications for ensialic rifting in the Middle Proterozoic of northwest Queensland: Precambrian Research, v. 40/41, p. 487–507.

Bell, R.T., 1978, Breccias and uranium mineralization in

the Wernecke Mountains, Yukon Territory—A progress report: Geological Survey of Canada, Paper 78-1A, p. 317–322.

Bell, R.T., 1986a, Megabreccias in northeastern Wernecke Mountains, Yukon Territory: Geological Survey of Canada, Paper 86-1A, p. 375–384.

Bell, R.T., 1986b, Geological map of northeastern Wernecke Mountains, Yukon Territory: Geological Survey of Canada, Open File 1207, scale: 1: 100 000.

Bell, R.T., and Delaney, G.D., 1977, Geology of some uranium occurrences in Yukon Territory: Geological Survey of Canada, Paper 77-1A, p. 33–37.

Betts, P.G., Lister, G.S., and O'Dea, M.G., 1998, Asymmetric extension of the Middle Proterozoic lithosphere, Mount Isa inlier, Queensland, Australia: Tectonophysics, v. 296, p. 293–316.

Betts, P.G., Giles, D., and Lister, G.S., 2003, Tectonic environment of shale-hosted massive sulfide Pb-Zn-Ag deposits of Proterozoic northeastern Australia: Economic Geology, v. 98, p. 3:557–3:576.

Blake, D.H., and Stewart, A.J., 1992, Stratigraphic and tectonic framework, Mount Isa inlier, *in* Stewart, A.J., and Blake, D.H., eds., Detailed studies of the Mount Isa inlier: Bureau of Mineral Resources, Australian Geological Survey Organisation (AGSO), Bulletin 243, p. 1–11.

Blake, D.H., Etheridge, M.A., Page, R.W., Stewart, A.J., Williams, P.R., and Wyborn, L.A.I., 1990, Mount Isa inlier—Regional geology and mineralization, *in* Hughes, F.E., ed., Geology of the mineral deposits of Australia and Papua New Guinea: Melbourne, Australasian Institute of Mining and Metallurgy, p. 915–925.

Brideau, M.-A., Thorkelson, D.J., Godin, L., and Laughton, J.R., 2002, Paleoproterozoic deformation of the Racklan orogeny, Slats Creek (106D/16) and Fairchild Lake (106C/13) map areas, Wernecke Mountains, Yukon, *in* Emond, D.S., Weston, L.H., and Lewis, L.L., eds., Yukon Exploration and Geology 2001: Exploration and Geological Services Division, Yukon Region, Indian and Northern Affairs Canada, p. 65–72.

Brooks, M., Baker, T., and Hunt, J., 2002, Alteration zonation, veining, and mineralization associated with the Wernecke Breccias at Slab creek, Yukon Territory, Canada, *in* Emond, D.S., Weston, L.H., and Lewis, L.L., eds., Yukon Exploration and Geology 2001: Exploration and Geological Services Division, Yukon Region, Indian and Northern Affairs Canada, p. 249–258.

Carlon, C.J., 2000, Iron oxide systems and base metal mineralization in northern Sweden, *in* Porter, T.M., ed., Hydrothermal iron oxide copper-gold and related deposits: A global perspective, Volume 1: Adelaide, PGC Publishing, p. 283–296.

Compston, D.M., 1995, Time constraints on the evolution of the Tennant Creek block, northern Australia: Precambrian Research, v. 71, p. 107–129.

Cox, S.F., and Ruming, K., 2004. The St. Ives mesothermal gold system, Western Australia; A case of golden aftershocks?: Journal of Structural Geology, v. 26, p. 1109–1125.

Creaser, R.A., 1995, Neodymium isotopic constraints for the origin of Mesoproterozoic felsic magmatism, Gawler craton, South Australia: Canadian Journal of Earth Science, v. 32, p. 460–471.

Cross, K.C., Daly, S.J., and Flint, R.B., 1993, Olympic Dam deposit: Geological survey of South Australia, Bulletin 54, v. 1, p. 132–138.

Davidson, G.J., Davis, B.K., and Garner, A., 2002, Structural and geochemical constraints on the emplacement of the Monakoff oxide Cu-Au (-Co-U-REE-Ag-Zn-Pb) deposit, Mt. Isa inlier, Australia, *in* Porter, T.M., ed., Hydrothermal iron oxide copper-gold and related deposits: A global perspective, Volume 2: Adelaide, PGC Publishing, p. 49–75.

Davis, T.P., 2004, Mine-scale structural controls on the Mount Isa Zn-Pb-Ag and Cu orebodies: Economic Geology, v. 99, p. 543–559.

De Jong, G., and Williams, P.J., 1995, Evolution of metasomatic features during exhumation of mid crustal Proterozoic rocks in the vicinity of the Cloncurry fault, NW Queensland: Australian Journal of Earth Sciences, v. 42, p. 281–290.

Delaney, G.D., 1981, The Mid-Proterozoic Wernecke Supergroup, Wernecke Mountains, Yukon Territory: Geological Survey of Canada, Paper 81-10, p. 1–23.

Deming, D., 1992, Catastrophic release of heat and fluid flow in the continental crust: Geology, v. 20, p. 83–86.

DOCEGEO, 1988, Revisão litoestratigráfica da Província Mineral de Carajás: Congresso Brasileiro de Geologia, 35, Belém, Anexo aos Anais, p. 11–56.

Einaudi, M.T., and Oreskes, N., 1990, Progress towards an occurrence model for Proterozoic iron oxide (Cu, U, REE, Au) deposits—A comparison between the ore provinces of South Australia and SE Missouri: US Geological Survey, Bulletin 1392, p. 58–69.

Eldridge, C.S., 1994, Low sulphur isotope ratios; high gold values—A closer look at the Olympic Dam deposit via SHRIMP[abs.]: Geological Society of America, 1994 Annual Meeting, Abstracts with Programs, p. A:498–A:499.

Ferris, G.M., Schwarz, M.P., and Heithersay, P., 2002, The geological framework, distribution, and controls of Fe oxide Cu-Au mineralization in the Gawler Craton, South Australia, Part 1—Geological and tectonic framework, *in* Porter, T.M., ed., Hydrothermal iron oxide copper-gold and related deposits: A global perspective, Volume 2: Adelaide, PGC Publishing, p. 9–31.

Fleischer, V.D., Garlick, W.G., and Haldane, R., 1976, Geology of the Zambian Copperbelt, *in* Wolf, K.H., ed., Handbook of stratabound and stratiform ore deposits: Amsterdam, Elsevier, p. 223–352.

Frietsch, R., Billström, K., and Perdahl, J.A., 1995, Sulphur isotopes in Lower Proterozoic iron and sulphide ores in northern Sweden: Mineralium Deposita, v. 30, p. 275–284.

Frietsch, R., Tuisku, P., Martinsson, O., and Perdahl, J., 1997, Early Proterozoic Cu(-Au) and Fe ore deposits associated with regional Na-Cl metasomatism in northern Fennoscandia: Ore Geology Reviews, v. 12, p. 1–34.

Gabrielse, H., 1967, Tectonic evolution of the northern

Canadian Cordillera: Canadian Journal of Earth Sciences, v. 4, p. 271–298.

Gandhi, S.S., and Bell, R.T., 1990, Metallogenic concepts to aid exploration for the giant Olympic Dam-type deposits and their derivatives [abs.]: 8th IAGOD Symposium, Ottawa, Canada, August 1990, Program with abstracts, p. A7.

Garven, G., Bull, S.W., and Large, R.R., 2001, Hydrothermal fluid flow models of stratiform ore genesis in the McArthur Basin, Northern Territory, Australia: Geofluids, v. 1, p. 289–311.

Goodfellow, W.D., 1979, Geochemistry of copper, lead, and zinc mineralization in Proterozoic rocks near Gillespie Lake, Yukon: Geological Survey of Canada, Paper 79-1A, p. 333–348.

Gorbatshev, R., and Bogdanova, S., 1993, Frontiers in the Baltic Shield: Precambrian Research, v. 64, p. 3–21.

Haynes, D.W., 2000, Iron oxide copper (-gold) deposits: Their position in the ore deposit spectrum and modes of origin, *in* Porter, T.M., ed., Hydrothermal iron oxide copper-gold and related deposits: A global perspective, Volume 1: Adelaide, PGC Publishing, p. 71–90.

Haynes, D.W., Cross, K.C., Bills, R.T., and Reed, M.H., 1995, Olympic Dam ore genesis: A fluid-mixing model: Economic Geology, v. 90, p. 281–307.

Heinrich, C.A., Andrew, A.S., Wilkins, R.W.T., and Patterson, D.J., 1989, A fluid inclusion and stable isotope study of synmetamorphic copper ore formation at Mount Isa, Australia: Economic Geology, v. 84, p. 529–550.

Heinrich, C.A., Bain, J.H.C., Fardy, J.J., and Waring, C., 1993, Bromine/chlorine geochemistry of hydrothermal brines associated with Proterozoic metasediment-hosted copper mineralization at Mount Isa, northern Australia: Geochimica Cosmochimica Acta, v. 57, p. 2991–3000.

Heinrich, C.A., Bain, J.H.C., Mernagh, T.P., Wyborn, L.A.I., Andrew, A.S., and Waring, C., 1995, Fluid and mass transfer during metabasalt alteration and copper mineralization at Mount Isa, Australia: Economic Geology, v. 90, p. 705–730.

Heinrich, C.A., Andrew, A.S., and Knill, M.D., 2000, Regional metamorphism and ore formation: Evidence from stable isotopes and other fluid tracers, *in* Spry, P.G. et al., eds., Metamorphosed and metamorphogenic ore deposits: Reviews in Economic Geology, v. 11, p. 97–117.

Hitzman, M.W., 2000, Iron oxide-Cu-Au deposits: What, where, when, and why?, *in* Porter, T.M., ed., Hydrothermal iron oxide copper-gold and related deposits: A global perspective, Volume 1: Adelaide, PGC Publishing, p. 9–25.

Hitzman, M.W., Oreskes, N., and Einaudi, M.T., 1992, Geological characteristics and tectonic setting of Proterozoic iron oxide (Cu-U-Au-REE) deposits: Precambrian Research, v. 58, p. 241–287.

Hunt, J.A., 2005, The geology and genesis of iron oxide copper-gold mineralisation associated with Wernecke Breccia, Yukon, Canada: Ph.D. Thesis, Townsville, Australia, James Cook University, 120 p.

Hunt, J.A., Laughton, J.R., Brideau, M.-A., Thorkelson, D.J., Brookes, M.L., and Baker, T., 2002, New mapping around the Slab iron oxide copper-gold occurrence, Wernecke Mountains, *in* Emond, D.S., Weston, L.H., and Lewis, L.L., eds., Yukon exploration and geology 2001: Exploration and Geological Services Division, Yukon Region, Indian and Northern Affairs Canada, p. 125–138.

Hunt, J.A., Baker, T., Davidson, G., Fallick, A.E., and Thorkelson, D.J., 2004, Origin of Wernecke Breccia: Results of fluid inclusion and stable isotope analyses [abs.]: Geological Society of Australia (GSA) Conference, Hobart, Tasmania, February 2004, Abstract, v. 73, p. 89.

Hunt, J.A., Baker, T., and Thorkelson, D.J., 2005, Regional-scale Proterozoic IOCG-mineralised breccia systems: Examples from the Wernecke Mountains, Yukon, Canada: Mineralium Deposita, v. 40, p. 492–514.

Huston, D.L., Bolger, C., and Cozens, G., 1993, A comparison of mineral deposits at the Gecko and White Devil deposits: Implications for ore genesis in the Tennant Creek district, Northern Territory, Australia: Economic Geology, v. 88, p. 1198–1225.

Jackson, M.J., and Southgate, P.N., 2000, Evolution of three unconformity-bounded sand-carbonate successions in the McArthur River region of Northern Australia: The Lawn, Wide and Doom Supersequences in a proximal part of the Isa Superbasin: Australian Journal of Earth Sciences, v. 47, p. 625–636.

Johnson, J.P., and Cross, K.C., 1991, Geochronological and Sm-Nd constraints on the genesis of the Olympic Dam Cu-U-Au-Ag deposit, South Australia, *in* Pagel, M., and Leroy, J.L., eds., Source, transport and deposition of metals: 25 Years' SGA Anniversary Meeting, Nancy, Aug. 30–Sept. 3, 1991, AA Balkema, Rotterdam, The Netherlands, Proceedings, p. 395–400.

Johnson, J.P., and Cross, K.C., 1995, U-Pb geochronological constraints on the genesis of the Olympic Dam Cu-U-Au-Ag deposit, South Australia: Economic Geology, v. 90, p. 1046–1063.

Knutson, J., Fergurson, J., Roberts, W.M.B., and Donnelly, T.H., 1979, Petrogenesis of copper-bearing breccia pipes, Redbank, Northern Territory, Australia: Economic Geology, v. 74, p. 814–826.

Knutson, J., Donnely, T.H., Eadington, P.J., and Tonkin, D.G., 1992, Hydrothermal alteration of Middle Proterozoic basalts, Stuart shelf, South Australia—A possible source for copper mineralization: Economic Geology, v. 87, p. 1054–1077.

Kwak, T.A.P., 1977, Scapolite compositional change in metamorphic gradient and its bearing on the identification of metaevaporite sequences: Geological Magazine, v. 114, p. 343–354.

Laing, W.P., 1998, Structural-metasomatic environment of the East Mount Isa Block base metal-gold province: Australian Journal of Earth Sciences, v. 45, p. 413–428.

Lane, R.A., 1990, Geologic setting and petrology of the Proterozoic Ogilvie Mountains breccia of the Coal Creek inlier, southern Ogilvie Mountains, Yukon Territory: M.Sc. Thesis, Vancouver, University of British

Columbia, 223 p.
Large, R.R., 1975, Zonation of hydrothermal minerals at the Juno mine, Tennant Creek goldfield, central Australia: Economic Geology, v. 70, p. 1387–1413.
Laughton, J.R., 2004, The Proterozoic Slab volcanics of northern Yukon, Canada: Megaclasts of a volcanic succession in Proterozoic Wernecke Breccia, and implications for the evolution of northwestern Laurentia: M.Sc. Thesis, Burnaby, British Columbia, Simon Fraser University, 200 p.
Laughton, J.R., Thorkelson, D.J., Brideau, M.-A., Hunt, J.A., and Marshall, D.D., 2005, Early Proterozoic orogeny and exhumation of Wernecke Supergroup revealed by vent facies of Wernecke Breccia, Yukon, Canada: Canadian Journal of Earth Sciences, v. 42, p. 1033–1044.
Lindenmayer, Z.G., 1990, Salobo sequence, Carajás, Brazil: Ph.D. Thesis, London, Canada, University of Western Ontario, 406 p.
Liu, W., and McPhail, D.C., 2005, Thermodynamic properties of copper chloride complexes and copper transport in magmatic-hydrothermal solutions: Chemical Geology, v. 221, p. 21–39.
Lowenstern, J.B., 2001, Carbon dioxide in magmas and implications for hydrothermal systems: Mineralium Deposita, v. 36, p. 490–502.
MacCready, T., Goleby, B.R., Goncharov, A., Drummond, B.J., and Lister, G.S., 1998, A framework of overprinting orogens based on the interpretation of the Mount Isa deep seismic transect: Economic Geology, v. 93, p. 1422–1434.
Machado, N., Lindenmayer, Z.G., Krogh, T.E., and Lindenmayer, D., 1991, U-Pb geochronology of Archean magmatism and basement reactivation in the Carajás area, Amazon Shield, Brazil: Precambrian Research, v. 49, p. 329–354.
Mark, G., and Crookes, R.A., 1999, A hydrothermal origin for the Ernest Henry Fe oxide-(Cu-Au) deposit, Cloncurry district, Australia, *in* Stanley, C.J., et al., eds., Mineral Deposits: Processes to processing: Rotterdam, Balkema, p. 235–238.
Mark, G., and De Jong, G., 1996, Synchronous granitoid emplacement and episodic sodic-calcic alteration in the Cloncurry district: Styles, timing, and metallogenic significance: Economic Geology Research Unit, James Cook University, Townsville, Australia, Contribution 55, p. 77–80.
Mark, G., Oliver, N.H.S., Williams, P.J., Valenta, R.K., and Crookes, R.A., 2000, The evolution of the Ernest Henry Fe-oxide-(Cu-Au) hydrothermal system, *in* Porter, T.M., ed., Hydrothermal iron oxide copper-gold and related deposits: A global perspective, Volume 1: Adelaide, PGC Publishing, p. 123–136.
Mark, G., Oliver, N.H.S., and Williams, P.J., 2006, Mineralogical and chemical evolution of the Ernest Henry Fe oxide-Cu-Au ore system, Cloncurry district, northwest Queensland, Australia: Mineralium Deposita, v. 40, p. 769–801.
Marschik, R., and Fontboté, L., 1996, Copper(-iron) mineralization and superposition of alteration events in the Punta del Cobre belt, northern Chile, *in* Camus, F., Sillitoe, R.H., Peterson, R., eds., Andean copper deposits: New discoveries, mineralization, styles, and metallogeny: Society of Economic Geologists, Special Publication 5, p. 171–190.
Marschik, R., and Fontboté, L., 2001, The Candelaria–Punta del Cobre iron oxide Cu-Au (-Zn-Ag) deposits, Chile: Economic Geology, v. 96, p. 1799–1826.
Marschik, R., Leveille, R.A., and Martin, W., 2000, La Candelaria and the Punta del Cobre district, Chile: Early Cretaceous iron oxide Cu-Au (-Zn-Ag) mineralization, *in* Porter, T.M., ed., Hydrothermal iron oxide copper-gold and related deposits: A global perspective, v. 1: Adelaide, PGC Publishing, p.163–175.
Marschik, R., Mathur, R., Ruiz, J., Leveille, R.A., and de Almeida, A.-J., 2005, Late Archean Cu-Au-Mo mineralization at Gameleira and Serra Verde, Carajàs mineral province, Brazil: Constraints from Re-Os molybdenite ages: Mineralium Deposita, v. 39, p. 983–991.
Mathur, R., Marschik, R., Ruiz, J., Munizaga, F., Leveille, R.A., and Martin, W., 2002, Age and mineralization of the Candelaria Fe oxide Cu-Au deposit and the origin of the Chilean iron belt, based on Re-Os isotopes: Economic Geology, v. 97, p. 59–71.
Matthai, S.K., Heinrich, C.A., and Driesner, T., 2004, Is the Mount Isa copper deposit the product of forced brine convection in the footwall of a major reverse fault?: Geology, v. 32, p. 357–360.
McGowan, R.R., Roberts, S., Foster, R.P., Boyce, A.J., and Coller, D., 2003, Origin of the copper-cobalt deposits of the Zambian Copperbelt: An epigenetic view from Nchanga: Geology, v. 31, p. 497–500.
McGowan, R.R., Roberts, S., and Boyce, A.J., 2006, Origin of the Nchanga copper-cobalt deposits of the Zambian Copperbelt: Mineralium Deposita, v. 40, p. 617–638.
McKibben, M.A., and Elders, W.A., 1985, Fe-Zn-Cu-Pb mineralization in the Salton Sea geothermal system, Imperial Valley, California: Economic Geology, v. 89, p. 539–559.
McKibben, M.A., and Hardie, L.A., 1997, Ore-forming brines in active continental rifts, *in* Barnes, H.L., ed., Geochemistry of hydrothermal ore deposits: New York, Wiley, p. 877–936.
Meyer, C., 1988, Proterozoic ore-forming habitats—Tectonic and chemical transitions, *in* Kisvarsanyi, G., and Grant, S.K., eds., Tectonic controls of ore deposits and vertical and horizontal extent of ore systems: Rolla, University of Missouri, October 6–8, 1987, Conference Proceedings, p. 217–235.
Monro, D., 1988, The geology and genesis of the Aitik copper-gold deposit, Arctic Sweden: Ph.D. Thesis, Cardiff College, University of Wales, U.K., 98 p.
Mustard, R., Baker, T., Williams, P., Ulrich, T., Mernagh, T., Ryan, C.G., VanAchterbergh, E., and Adshead, N., 2003, Cu-rich brines at the Osborn and Starra deposits: Implications for immiscibility in Fe-oxide Cu-Au systems: Applied Earth Science Transactions of the Institute of Mining and Metallurgy, Section B, v. 112,

p. B189–B191.
O'Dea, M.G., Lister, G.S., and MacCready, T., 1997, Geodynamic evolution of the Proterozoic Mount Isa Terrain, in Burg, J.-P., and Ford, M., eds., Orogeny through time: Geological Society of London, Special Publication 121, p. 99–122.
Ohmoto, H., and Goldhaber, M.B., 1997, Sulfur and carbon isotopes, *in* Barnes, H.L., ed., Geochemistry of hydrothermal ore deposits, 2nd ed.: New York, Wiley, p. 517–612.
Oreskes, N., and Einaudi, M.T., 1990, Origin of REE-enriched hematite breccias at the Olympic Dam Cu-U-Au-Ag deposit, Roxby Downs, South Australia: Economic Geology, v. 85, p. 1–28.
Oreskes, N., and Einaudi, M.T., 1992, Origin of hydrothermal fluids at Olympic Dam: Preliminary evidence from fluid inclusions and stable isotopes: Economic Geology, v. 87, p. 64–88.
Oreskes, N., and Hitzman, M.W., 1993, A model for the origin of Olympic Dam-type deposits, *in* Kirkham, R.V., Sinclair, W.D., Thorpe, R.I., and Duke, J.M., eds., Mineral deposit modeling: Geological Association of Canada, Special Paper 40, p. 615–633.
Orridge, G.R., and Mason, A.A.C., 1975, Redbank copper deposits, *in* Knight, C.L., ed., Economic geology of Australia and Papua New Guinea, Part 1—Metals: Australian Institute of Mining and Metallurgy, Monograph 5, p. 339–343.
Page, R.W., and Sun, S.-S., 1998, Aspects of geochronology and crustal evolution in the Eastern fold belt, Mount Isa inlier: Australian Journal of Earth Sciences, v. 45, p. 343–361.
Perkins, C., 1990, Mount Isa copper orebodies, *in* Hughes, F.E., ed., Geology of the mineral deposits of Australia and Papua New Guinea: Australasian Institute of Mining and Metallurgy, Monograph 14, p. 935–941.
Perkins, C., Heinrich, C.A., and Wyborn, L.A.I., 1999, $^{40}Ar/^{39}Ar$ geochronology of copper mineralization and regional alteration, Mount Isa, Australia: Economic Geology, v. 94, p. 23–36.
Perkins, W.G., 1984, Mount Isa silica dolomite and copper orebodies: The result of a syntectonic hydrothermal system: Economic Geology, v. 79, p. 601–637.
Perring, C.S., Pollard, P.J., Dong, G., Nunn, A.J., and Blake, K.L., 2000, The Lightening Creek sill complex, Cloncurry district, northwest Queensland: A source of fluids for Fe oxide Cu-Au mineralization and sodic-calcic alteration: Economic Geology, v. 95, p. 1067–1090.
Pinheiro, R.V.L., 1997, Reactivation history of the Carajás and Cinzento strike-slip systems, Amazon, Brazil: Ph.D. Thesis, University of Durham, U.K, 408 p.
Pollard, P.J., 2000, Evidence of a magmatic fluid and metal source for Fe oxide Cu-Au mineralization, *in* Porter, T.M., ed., Hydrothermal iron oxide copper-gold and related deposits: A global perspective, Volume 1: Adelaide, PGC Publishing, p. 27–41.
Pollard, P.J., 2001, Sodic(-calcic) alteration in Fe oxide-Cu-Au districts: An origin via unmixing of magmatic-derived H_2O–CO_2–NaCl ± $CaCl_2$–KCl fluids: Mineralium Deposita, v. 36, p. 93–100.
Pollard, P.J., Mark, G., and Mitchell, L., 1998, Geochemistry of post-1540 Ma granites in the Cloncurry district: Economic Geology, v. 93, p. 1330–1344.
Raymond, J., 1995, Petrology: The study of igneous, metamorphic, and sedimentary rocks: New York, McGraw-Hill, 742 p.
Raymond, J., 2000, Mantle of the earth, *in* Sigurdsson, H., ed., Encyclopedia of volcanoes: San Diego, U.S., Academic Press, p. 41–54.
Reeve, J.S., Cross, K.C., Smith, R.N., and Oreskes, N., 1990, Olympic Dam copper-uranium-gold-silver deposit, *in* Hughes, F.E., ed., Geology of the mineral deposits of Australia and Papua New Guinea: Australasian Institute of Mining and Metallurgy, Monograph 14, p. 1009–1035.
Requia, K., and Fontboté, L., 2000, The Salobo iron oxide copper-gold deposit, Carajás, northern Brazil, *in* Porter, T.M., ed., Hydrothermal iron oxide copper-gold and related deposits: A global perspective, Volume 1: Adelaide, PGC Publishing, p. 225–236.
Requia, K., Stein, H., Fontboté, L., and Chiaradia, M., 2003, Re–Os and Pb–Pb geochronology of the Archean Salobo iron oxide copper-gold deposit, Carajás mineral province, northern Brazil: Mineralium Deposita, v. 38, p. 727–738.
Reynolds, L.J., 2000, Geology of the Olympic Dam Cu-U-Au-Ag-REE deposit, *in* Porter, T.M., ed., Hydrothermal iron oxide copper-gold and related deposits: A global perspective, Volume 1: Adelaide, PGC Publishing, p. 93–104.
Roberts, D.E., and Hudson, G.R.T., 1983, The Olympic Dam copper-uranium-gold deposit, Roxby Downs, South Australia: Economic Geology, v. 78, p. 799–822.
Roberts, D.E., and Hudson, G.R.T., 1984, The Olympic Dam copper-uranium-gold deposit, Roxby Downs, South Australia—A reply: Economic Geology, v. 79, p. 1944–1945.
Rollinson, H., 1993, Using geochemical data: Evaluation, presentation, interpretation: Harlow, United Kingdom, Longman Group, 352 p.
Ronzê, P.C., Soares, A.D.V., Giovanni, S., and Berreira, C.F., 2000, Alemão copper-gold (U-REE) deposit, Carajás, Brazil, *in* Porter, T.M., ed., Hydrothermal iron oxide copper-gold and related deposits: A global perspective, Volume 1: Adelaide, PGC Publishing, p. 191–202.
Rotherham, J.F., Blake, K.L., Cartwright, I., and Williams, P.J., 1998, Stable isotope evidence for the origin of the Mesoproterozoic Starra Cu-Au deposit, Cloncurry district, northwest Queensland: Economic Geology, v. 93, p. 1435–1449.
Ryan, A., 1998, Ernest Henry copper-gold deposit: Australasian Institute of Mining and Metallurgy, Monograph 22, p. 759–768.
Scott, D.L., Rawlings, D.J., Page, R.W., Tarlowski, C.Z., Idnurm, M., Jackson, M.J., and Southgate, P.N., 2000, Basement framework and geodynamic evolution of the Paleoproterozoic superbasins of north-central Australia: An integrated review of geochemical, geochronological,

and geophysical data: Australian Journal of Earth Sciences, v. 47, p. 341–380.

Sheppard, S.M.F., 1986, Characterization and isotopic variations in natural waters, *in* Valley, J.W., Taylor, H.P. Jr., and O'Neil, J.R., eds., Stable isotopes in high-temperature geological processes: Reviews in Mineralogy, Mineralogical Society of America, v. 16, p. 165–183.

Sillitoe, R.H., 2003, Iron oxide copper-gold deposits: An Andean view: Mineralium Deposita, v. 38, p. 787–812.

Skiöld, T., 1987, Aspects of Proterozoic geochronology on northern Sweden: Precambrian Research, v. 35, p. 161–167.

Skiöld, T., and Cliff, R.A., 1984, Sm–Nd and U–Pb dating of Early Proterozoic mafic-felsic volcanism in northernmost Sweden: Precambrian Research, v. 26, p. 1–13.

Skirrow, R.G., 1999, Proterozoic Cu-Au-Fe mineral systems in Australia: Filtering key components in exploration models, *in* Stanley, C.J., et al., eds., Mineral deposits: Processes to processing: Rotterdam, Balkema, p. 1361–1364.

Skirrow, R.G., and Walshe, J.L., 2002, Reduced and oxidized Au-Cu-Bi iron oxide deposits of the Tennant Creek Inlier, Australia: An integrated geologic and chemical model: Economic Geology, v. 97, p. 1167–1202.

Southgate, P.N., Bradshaw, B.E., Domagala, J., Jackson, M.J., Idurnam, M., Krassay, A.A., Page, R.W., Sami, T.T., Scott, D.L., Lindsay, J.F., McConachie, B.A., and Tarlowski, C., 2000, Chronostratigraphic basin framework for Paleoproterozoic rocks (1730–1575 Ma) in northern Australia and implications for base-metal mineralization: Australian Journal of Earth Sciences, v. 47, p. 461–483.

Souza, L.H., and Vieira, E.A., 2000, Salobo 3 alpha deposit: Geology and mineralization, *in* Porter, T.M., ed., Hydrothermal iron oxide copper-gold and related deposits: A global perspective, Volume 1: Adelaide, PGC Publishing, p. 213–224.

Sverjensky, D.A., 1987, The role of migrating oil-field brines in the formation of sediment-hosted copper-rich deposits: Economic Geology, v. 82, p. 1130–1141.

Swager, C.P., 1985, Syndeformational carbonate-replacement model for the copper mineralization at Mount Isa, Queensland: A microstructural study: Economic Geology, v. 80, p. 107–125.

Sweeney, M.A., Turner, P., and Vaughan, D.J., 1986, Stable isotope and geochemical studies of the role of early diagenesis in ore formation, Konkola Basin, Zambian Copperbelt: Economic Geology, v. 81, p. 1836–1852.

Tazava, E., and de Olivera, C.G., 2000, The Igarape Bahia Au-Cu(-REE-U) deposit, Carajás mineral province, northern Brazil, *in* Porter, T.M., ed., Hydrothermal iron oxide copper-gold and related deposits: A global perspective, Volume 1: Adelaide, PGC Publishing, p. 203–212.

Thorkelson, D.J., 2000, Geology and mineral occurrences of the Slats Creek, Fairchild Lake and "Dolores Creek" areas, Wernecke Mountains, Yukon Territory: Exploration and Geological Services Division, Yukon Region, Indian and Northern Affairs Canada, Bulletin 10, 73 p.

Thorkelson, D.J., Mortensen, J.K., Davidson, G.J., Creaser, R.A., Perez, W.A., and Abbott, J.G., 2001a, Early Mesoproterozoic intrusive breccias in Yukon, Canada: The role of hydrothermal systems in reconstructions of North America and Australia: Precambrian Research, v. 111, p. 31–55.

Thorkelson, D.J., Mortensen, J.K., Creaser, R.A., Davidson, G.J., and Abbott, J.G., 2001b, Early Proterozoic magmatism in Yukon, Canada: Constraints on the evolution of northwestern Laurentia: Canadian Journal of Earth Science, v. 38, p. 1479–1494.

Thorkelson, D.J., Laughton, J.R., and Hunt, J.A., 2002, Geological map of Quartet Lakes area (106E/1), Wernecke Mountains, Yukon: Exploration and Geological Services Division, Yukon Region, Indian and Northern Affairs Canada, Geoscience map 2002-2, scale 1:50 000.

Thorkelson, D.J., Laughton, J.R., Hunt, J.A., and Baker, T., 2003, Geology and mineral occurrences of the Quartet Lakes map area (NTS 106E/1), Wernecke and Mackenzie Mountains, Yukon, *in* Emond, D.S., and Lewis, L.L., eds., Yukon exploration and geology 2002: Exploration and Geological Services Division, Yukon Region, Indian and Northern Affairs Canada, p. 223–239.

Torgersen, T., 1990, Crustal-scale fluid transport, magnitude, and mechanisms: EOS, v. 71, p. 1, 4, 13.

Twyerould, S.C., 1997, The geology and genesis of the Ernest Henry Fe-Cu-Au deposit, northwest Queensland, Australia: Ph.D. Thesis, Eugene, U.S., University of Oregon, 494 p.

Ullrich, T.D., and Clark, A.H., 1999, The Candelaria copper-gold deposit, Region III, Chile: Paragenesis, geochronology, and fluid composition, *in* Stanley, C.J., et al., eds., Mineral deposits: Processes to processing, Volume 1: Proceedings of the 5th Biennial SGA Meeting and 10th Quadrennial IAGOD Symposium, London, UK, AA Balkema, Rotterdam, p. 201–204.

Unrug, R., 1988, Mineralization controls and source of metals in the Lufilian fold belt, Shaba (Zaire), Zambia, and Angola: Economic Geology, v. 83, p. 1247–1258.

Villas, R.N., and Santos, M.D., 2001, Gold deposits of the Carajàs mineral province: Deposit types and metallogenesis: Mineralium Deposita, v. 36, p. 300–331.

Wanhainen, C., and Martinsson, O., 1999, Geochemical characteristics of host rocks to the Aitik Cu-Au-Ag deposit, Gellivare area, northern Sweden, *in* Stanley, C.J., et al., eds., Mineral deposits: Processes to processing: Proceedings of the 5th Biennial SGA Meeting and 10th Quadrennial IAGOD Symposium, London, UK, AA Balkema, Rotterdam, p. 1443–1446.

Wanhainen, C., Broman, C., and Martinsson, O., 2003, The Aitik Cu-Au-Ag deposit in northern Sweden: A product of high-salinity fluids: Mineralium Deposita, v. 38, p. 715–726.

Wedekind, M.R., and Love, R.J., 1990, Warrego gold-copper-bismuth deposit, *in* Hughes, F.E., ed., Geology of the mineral deposits of Australia and Papua New Guinea: Melbourne, The Australian Institute of Mining and Metallurgy, p. 839–843.

Wilkins, J., Beane, R.E., and Heidrick, T.L., 1986, Mineralization related to detachment faults: A model: Arizona Geological Society Digest, v. XVI, p. 108–117.

Williams, P.J., and Blake, K.L., 1993, Alteration in the Cloncurry district: Roles of recognition and interpretation on exploration for Cu-Au and Pb-Zn-Ag deposits: Economic Geology Research Unit, Contribution 49, James Cook University, Australia, 75 p.

Williams, P.J., and Skirrow, R.G., 2000, Overview of iron oxide copper-gold deposits in the Curnamona province and Cloncurry district (eastern Mount Isa block), Australia, *in* Porter, T.M., ed., Hydrothermal iron oxide copper-gold and related deposits: A global perspective, Volume 1: Adelaide, PGC Publishing, p. 105–122.

Williams, P.J., and Pollard, P.J., 2003, Australian Proterozoic iron oxide-Cu-Au deposits: An overview with new metallogenic and exploration data from the Cloncurry district, northwest Queensland: Exploration and Mining Geology, v. 10, p. 191–213.

Williams, P.J., Dong, G., Pollard, P.J., and Perring, C.S., 1999, Fluid inclusion geochemistry of Cloncurry (Fe)-Cu-Au deposits, *in* Stanley, C.J., et al., eds., Mineral deposits: Processes to processing, Volume 1: Proceedings of the 5th Biennial SGA Meeting and 10th Quadrennial IAGOD Symposium, London, UK, AA Balkema, Rotterdam, p. 111–114.

Williams, P.J., Barton, M.D., Johnson, D.A., Fontboté, L., de Haller, A., Mark, G., Oliver, N.H.S., 2005, Iron oxide copper-gold deposits: Geology, space-time distribution, and possible modes of origin: Economic Geology, 100th Anniversary volume, Society of Economic Geologists, p. 371–405.

Wyborn, L.A., 1998, Younger ca. 1500 Ma granites of the Williams and Naraku batholiths, Cloncurry district, eastern Mount Isa Inlier: Geochemistry, origin, metallogenic significance, and exploration indicators: Australian Journal of Earth Sciences, v. 45, p. 397–411.

Yardley, B.W.D., and Graham, J.T., 2002, The origins of salinity in metamorphic fluids: Geofluids, v. 2, p. 249–256.

Yukon MINFILE, 2007, Database of Yukon mineral occurrences: Exploration and Geological Services Division, Yukon Region, Indian and Northern Affairs Canada, CD-ROM (2).